Heidelberg Institute for Theoretical Studies

HITS

# Gravitational waves from neutron-star mergers

ESNT workshop – Nucleosynthesis and equation of state of nuclear matter

CEA Saclay, 08/12/2017


Andreas Bauswein (Heidelberg Institute for Theoretical Studies)

With R. Ardevol, K. Chatziioannou, J. A. Clark, S. Goriely, H.-T. Janka, O. Just, N. Stergioulas


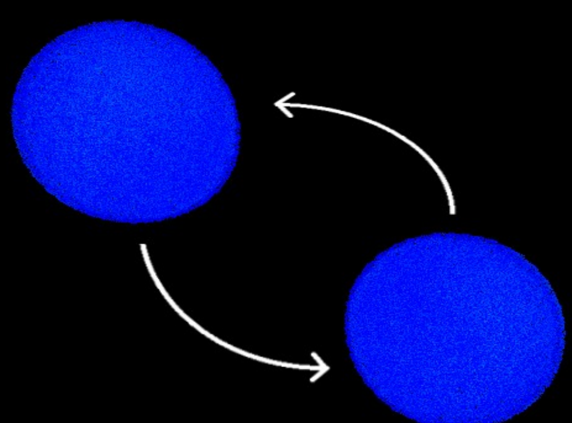

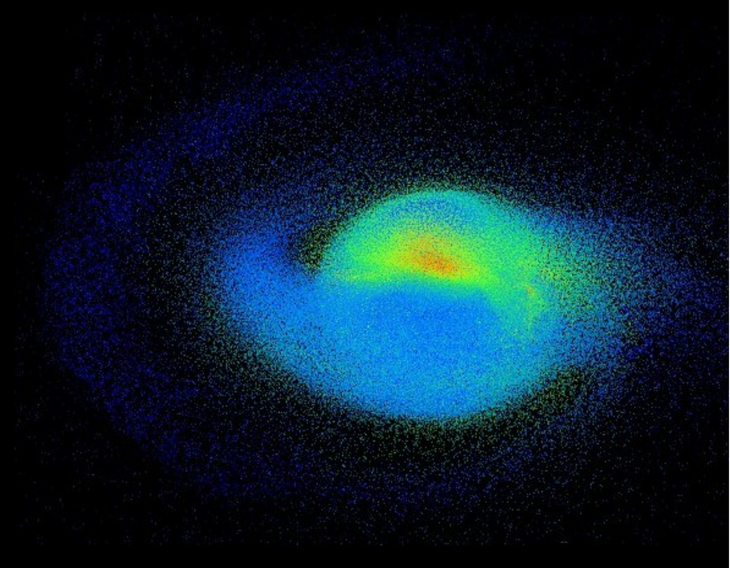

# Outline

- Introduction and Motivation
- Some insights from GW170817
- EoS constraints from NS mergers

  → tidal effects during inspiral

  → postmerger oscillation frequencies

  → GW data analysis aspects

  → unified picture of postmerger dynamics and GW emission

  → collapse behavior
- Summary and conclusions

# Introduction

- GW170817 first unambiguously detected NS merger
- Mutli-messenger observations: gravitational waves, gamma, X-rays, UV, optical, IR, radio
- NS mergers as progenitors of short gamma-ray bursts
- NS mergers as sources of heavy elements forged by the rapid neutron-capture process (→ see Stephane's talk)
- Electromagnetic transient powered by nuclear decays during/after r-process → UV, optical, IR → targets for triggered or blind searches (time-domain astronomy)
- Various other types of em counterparts
- Strong emitters of GWs

  → population properties: masses, rates, ... → stellar astrophysics

  → EoS of nuclear matter / stellar properties of NSs
- ...

# EoS of NS matter

- Mass-radius relation (of non-rotating NSs) and EoS are uniquely linked through Tolman-Oppenheimer-Volkoff (TOV) equations

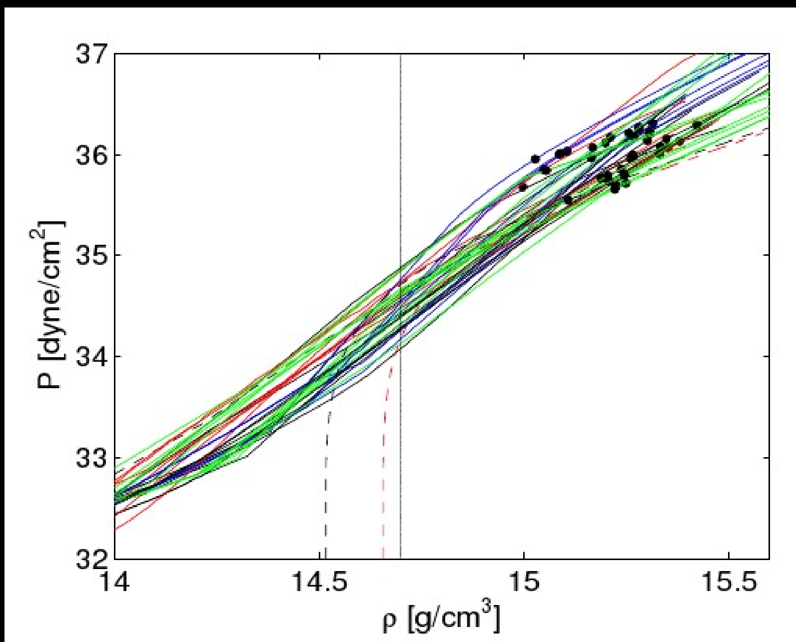


TOV

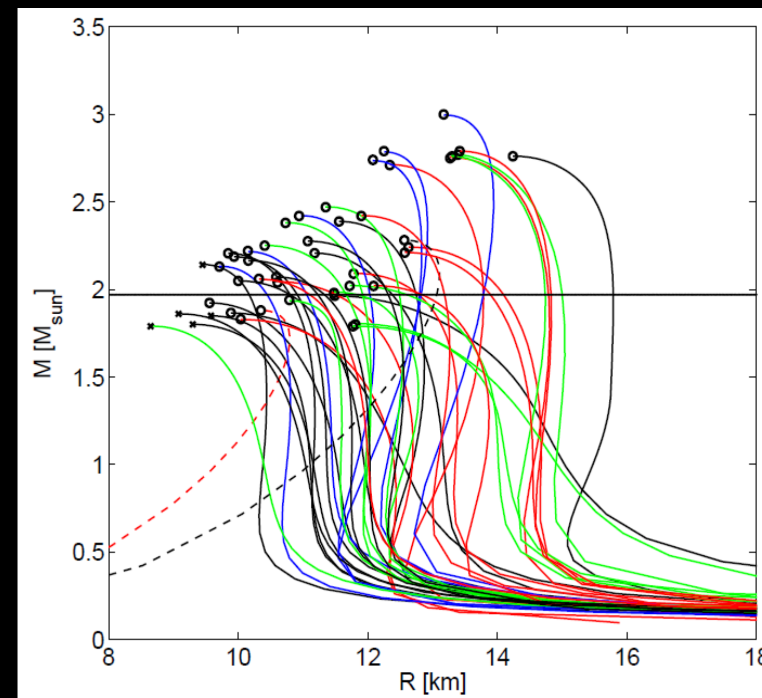


Theory: P(ρ) ⟷ Observation: R(M)

currently

future

=> NS properties (of non-rotating stars) and EoS properties are equivalent !!!

=> in particular we would like to measure radius of fixed mass, e.g. $R_{1.35}$, $R_{1.6}$

Maybe not all EoS compatible with all nuclear physics constraints

GW170817

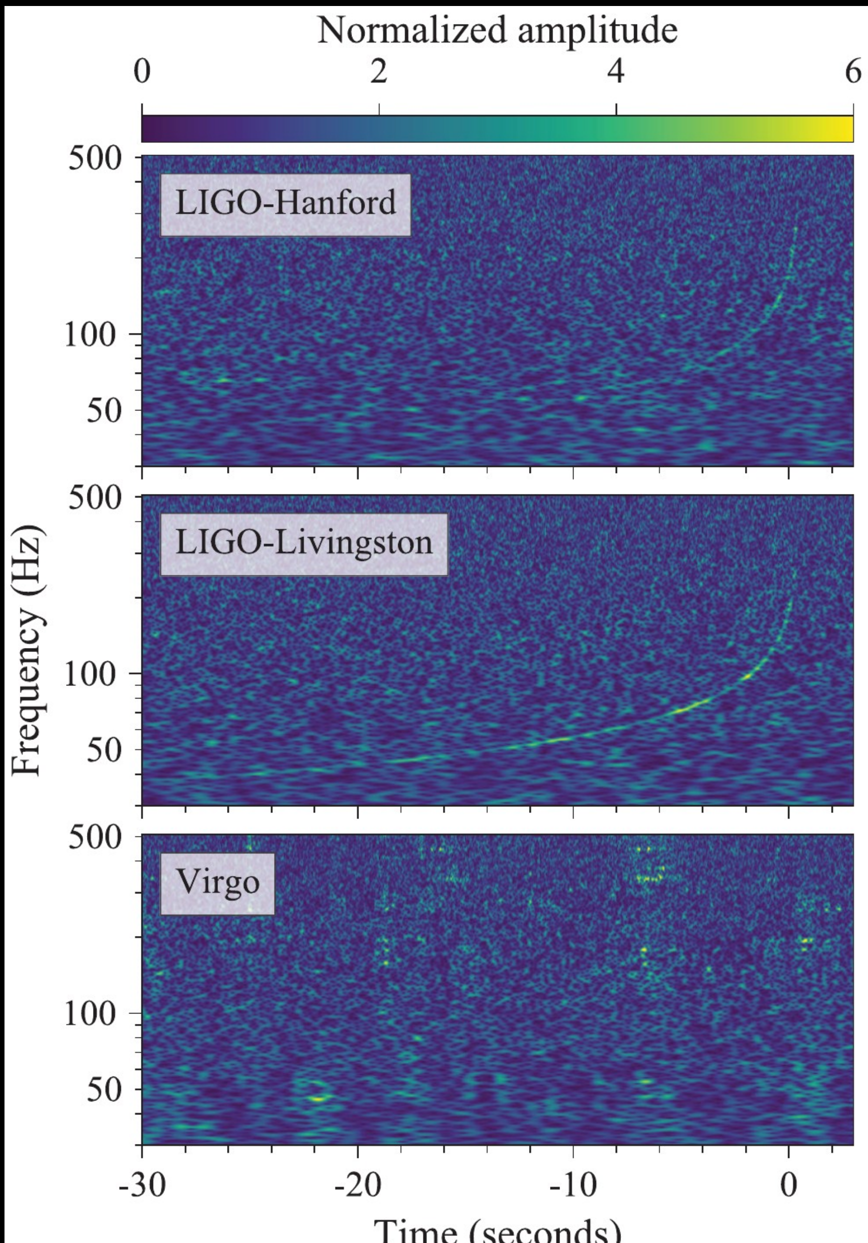


| | Low-spin priors ($\lvert\chi\rvert \leq 0.05$) |
|---|---|
| Primary mass $m_1$ | 1.36–1.60 $M_\odot$ |
| Secondary mass $m_2$ | 1.17–1.36 $M_\odot$ |
| Chirp mass $\mathcal{M}$ | $1.188^{+0.004}_{-0.002} M_\odot$ |
| Mass ratio $m_2/m_1$ | 0.7–1.0 |
| Total mass $m_{\mathrm{tot}}$ | $2.74^{+0.04}_{-0.01} M_\odot$ |
| Radiated energy $E_{\mathrm{rad}}$ | $> 0.025 M_\odot c^2$ |
| Luminosity distance $D_{\mathrm{L}}$ | $40^{+8}_{-14}$ Mpc |
| Viewing angle $\Theta$ | $\leq 55°$ |
| Using NGC 4993 location | $\leq 28°$ |
| Combined dimensionless tidal deformability $\tilde{\Lambda}$ | $\leq 800$ |
| Dimensionless tidal deformability $\Lambda(1.4 M_\odot)$ | $\leq 800$ |

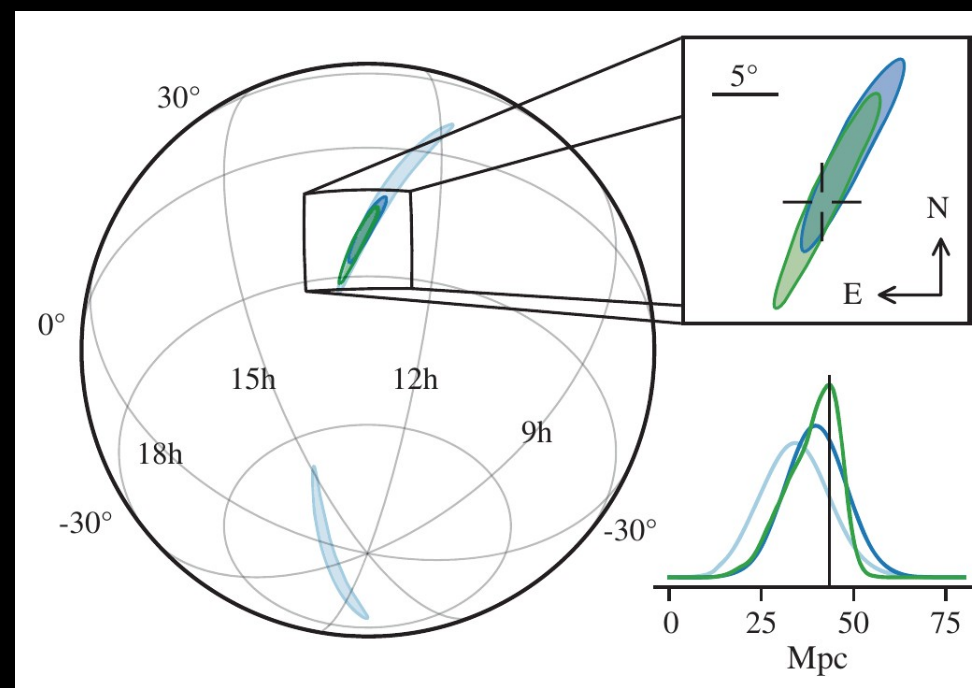


→ triggered some follow-up observations

Abbott et al 2017

# Some insights from GW170817

- Binary masses measured from inspiral
- Detection at 40 Mpc → rate is presumably high !
- Gamma-ray burst (?) followed 1.7 sec after GWs – but sub-luminous (by orders of magnitude) → different interpretations (off-axis, cocoon, choked, ...)
- Em counterpart: light curve compatible with ~0.05 Msun ejecta heated by r-process material

  - different components: blue and red (opacities of heavy r-process elements high)

  - interpretation somewhat model dependent

  - overall good agreement between observations and theoretical expectations

  → NS mergers are very very likely the source of r-process elements

  ( rate * ejecta mass sufficiently high to account for Galactic r-process inventory)

# Observations

- Follow up observation

  → ejecta masses, velocities

  → red and blue component

  → spectral features of heavy elements (?)

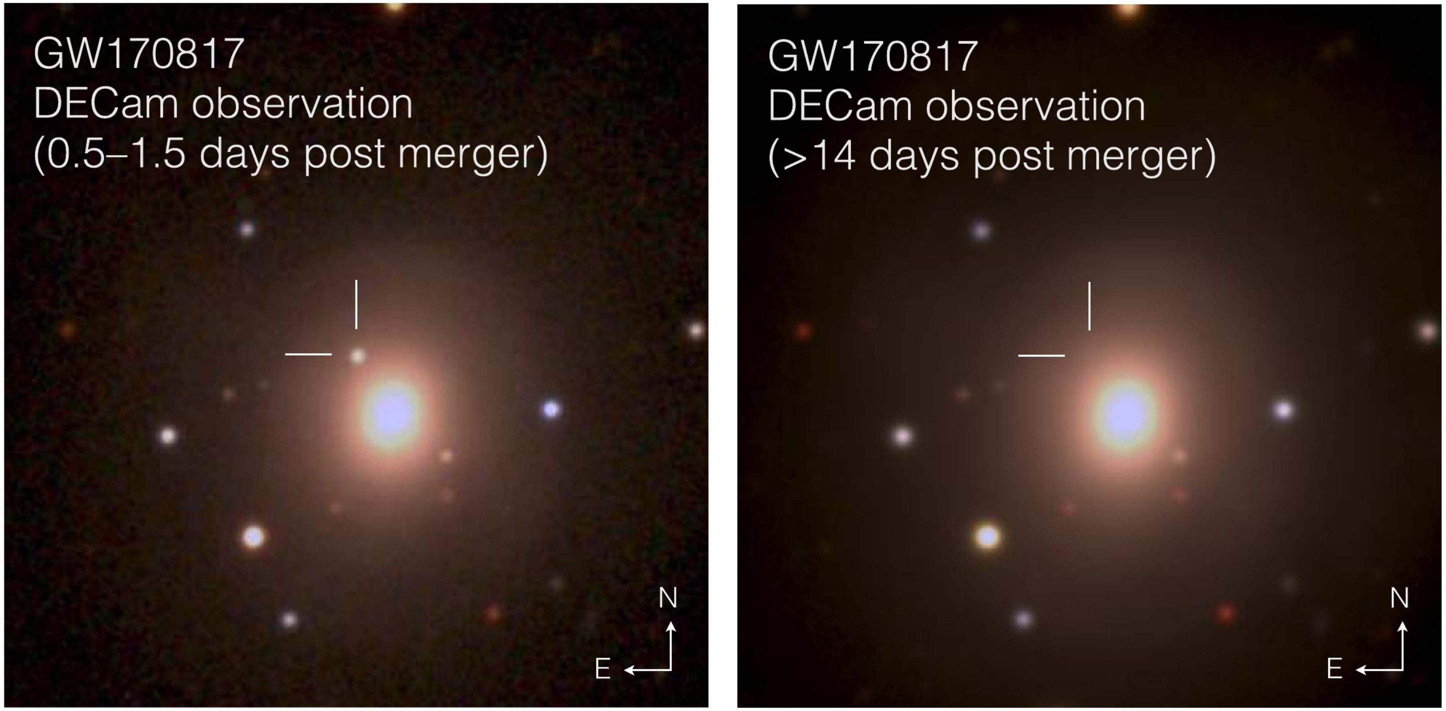


**Figure 1.** NGC4993 *grz* color composites (1.′5 × 1.′5). Left: composite of detection images, including the discovery *z* image taken on 2017 August 18 00:05:23 UT and the g and r images taken 1 day later; the optical counterpart of GW170817 is at R.A., decl. =197.450374, −23.381495. Right: the same area two weeks later.

Soares-Santos et al 2017

# Observations

- Light curves and derived ejecta masses

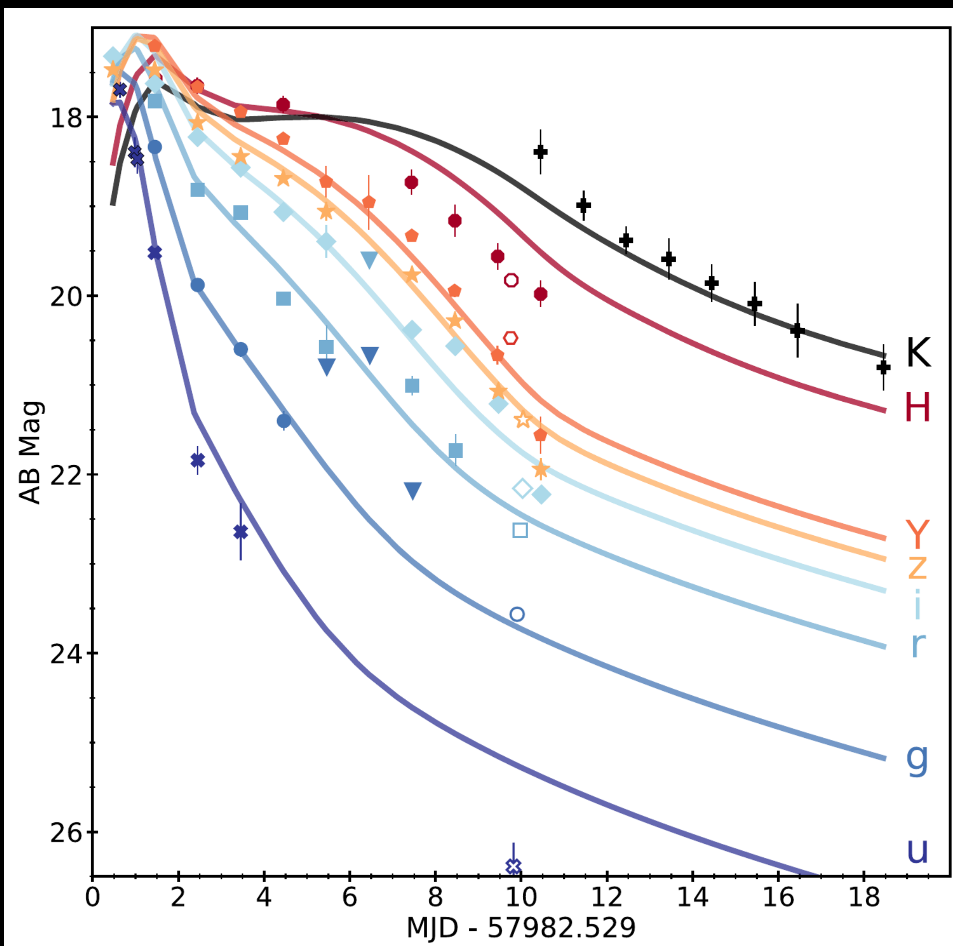


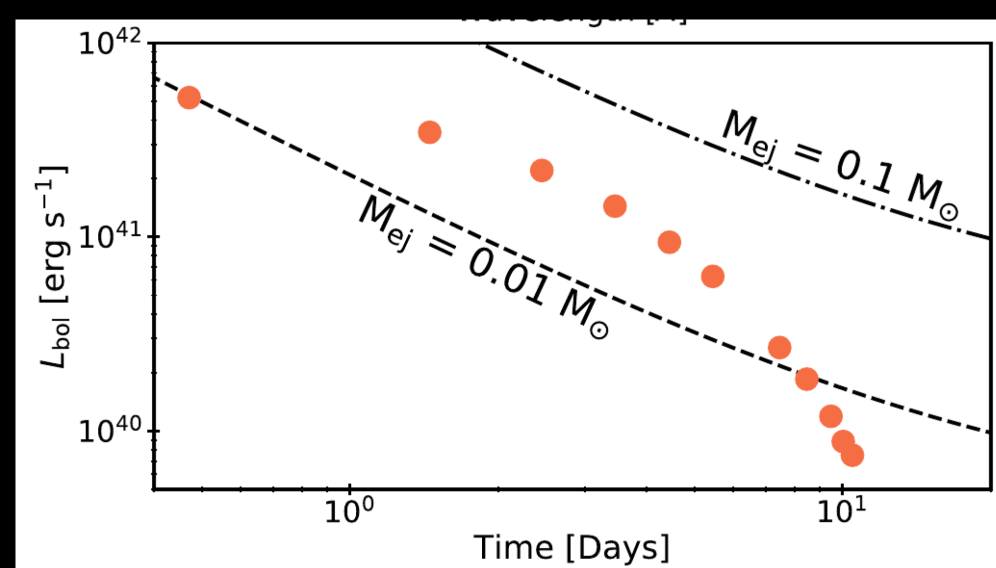


Interpreted as mutli-component outflow

Fast blue 0.01 $M_{sun}$ + slower red 0.04 $M_{sun}$

Cowperthwaite et al. 2017 (DECam, Gemini-South, HST observations)

# Observations

- Many IR/opt/UV observations by many groups
- Different interpretations / modeling
- Derived total ejecta masses all in the range 0.03 … 0.05 Msun

Chronock et al. 2017, Levan & Tanvir 2017, Kasliwal et al. 2017, Coulter et al. 2017, Allam et al. 2017, Yang et al. 2017, Arcavi et al. 2017, Kilpatrick et al. 2017, McCully et al. 2017, Pian et al. 2017, Arcavi et al. 2017, Evans et al. 2017, Drout et al. 2017 Lipunov et al. 2017, Cowperthwaite et al. 2017, Smarrt et al. 2017, Shappee et al. 2017, Nicholl et al. 2017, Kasen et al. 2017, Tanaka et al. 2017, …..

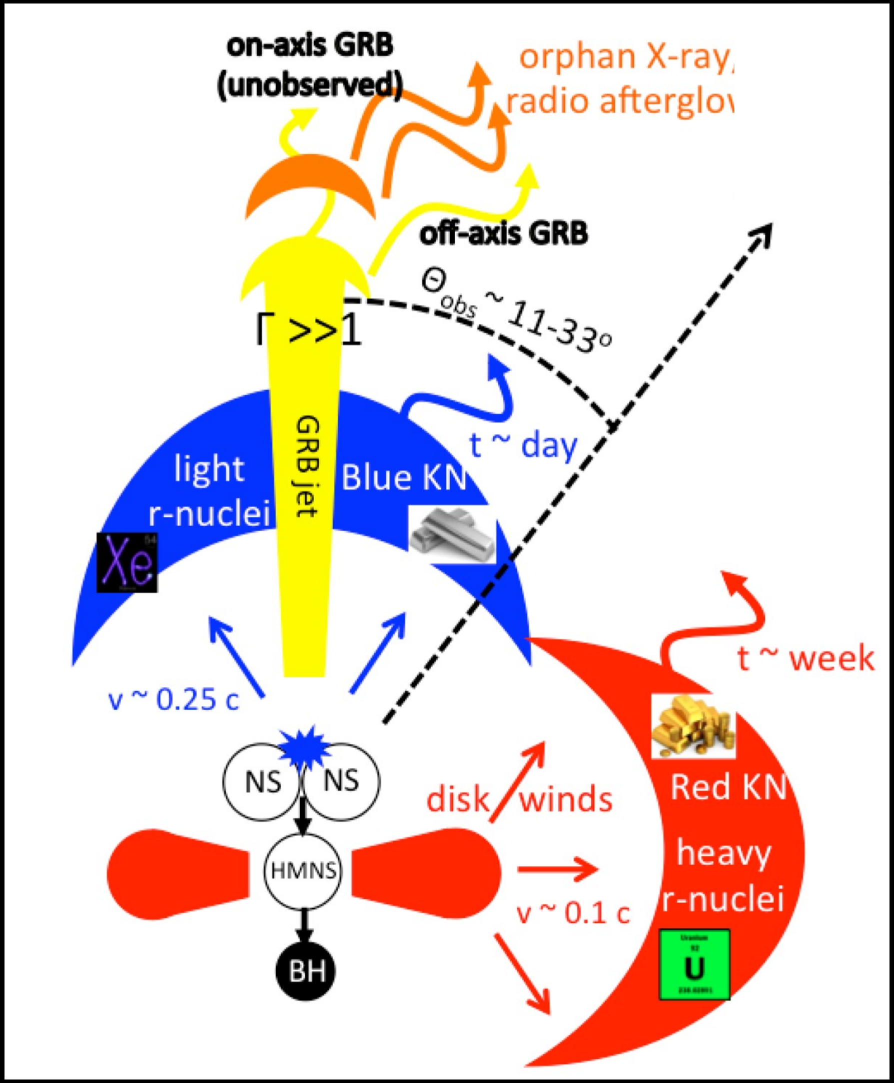


Metzger 2017

# Interpretation - implications

- heating and derived opacities are compatible with r-processing ejecta !!!

  (not surprising for a theorist)

- Derived velocities high → r-processing theoretically expected (unless proton-rich)
- Derived ejecta masses are compatible with mergers being the main source of heavy r-process elements in the Universe
- + indications for spectral features of heavy elements


® Made by NSM

# Mass measurements

$$M_{chirp} = \frac{(M_1 M_2)^{3/5}}{(M_1 + M_2)^{1/5}}$$

$$M_{tot} = M_1 + M_2$$

→ Chirp mass determines $M_{tot}$ quite well

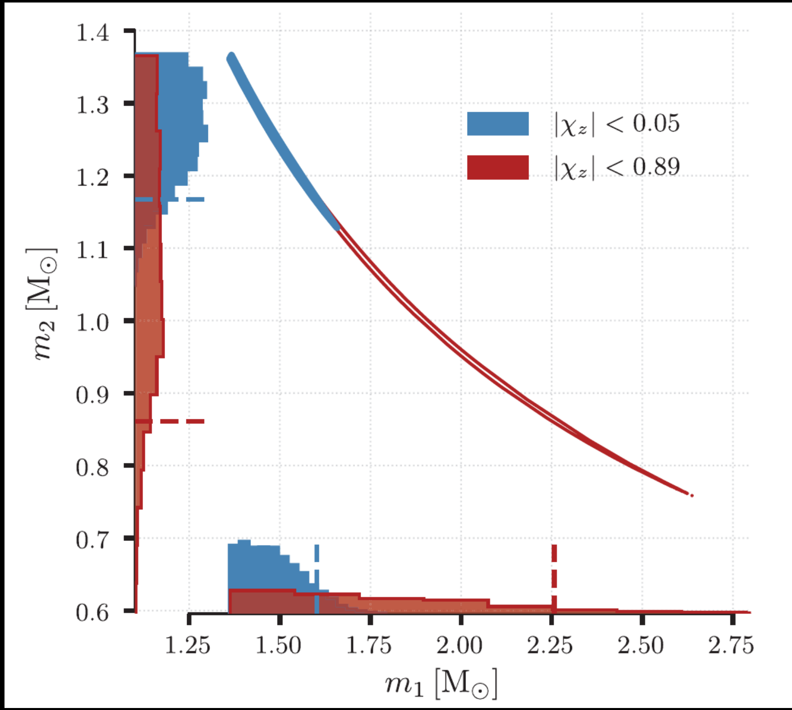


Abbott et al. 2017

| | Low-spin priors ($\|\chi\| \leq 0.05$) |
|---|---|
| Primary mass $m_1$ | 1.36–1.60 $M_\odot$ |
| Secondary mass $m_2$ | 1.17–1.36 $M_\odot$ |
| Chirp mass $\mathcal{M}$ | $1.188^{+0.004}_{-0.002} M_\odot$ |
| Mass ratio $m_2/m_1$ | 0.7–1.0 |
| Total mass $m_{\mathrm{tot}}$ | $2.74^{+0.04}_{-0.01} M_\odot$ |
| Radiated energy $E_{\mathrm{rad}}$ | $> 0.025 M_\odot c^2$ |
| Luminosity distance $D_{\mathrm{L}}$ | $40^{+8}_{-14}$ Mpc |
| Viewing angle $\Theta$ | $\leq 55°$ |
| Using NGC 4993 location | $\leq 28°$ |
| Combined dimensionless tidal deformability $\tilde{\Lambda}$ | $\leq 800$ |
| Dimensionless tidal deformability $\Lambda(1.4 M_\odot)$ | $\leq 800$ |

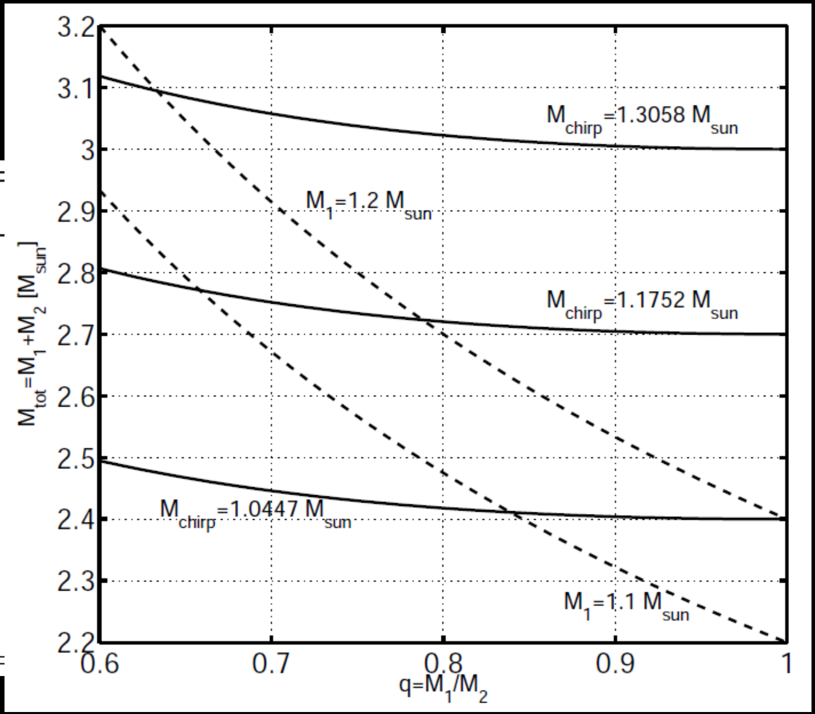


Minimum NS mass 1.1 - 1.2 Msun (e.g. Ertl et al. 2015 or measured masses)

# EoS constraints

(different approaches)

# Goal: EoS from GWs

Three complementary strategies:

- Tidal effects during the inspiral → accelerate inspiral compared to BH-BH

  - strong signal – weaker EoS effect

- Oscillations of the postmerger remnant

  - strong EoS impact – weaker signal (at higher frequencies)

- Collapse behavior

(keep in mind binary masses are easy to measure, i.e. at low SNR !!!)

# Finite-size effects during late inspiral

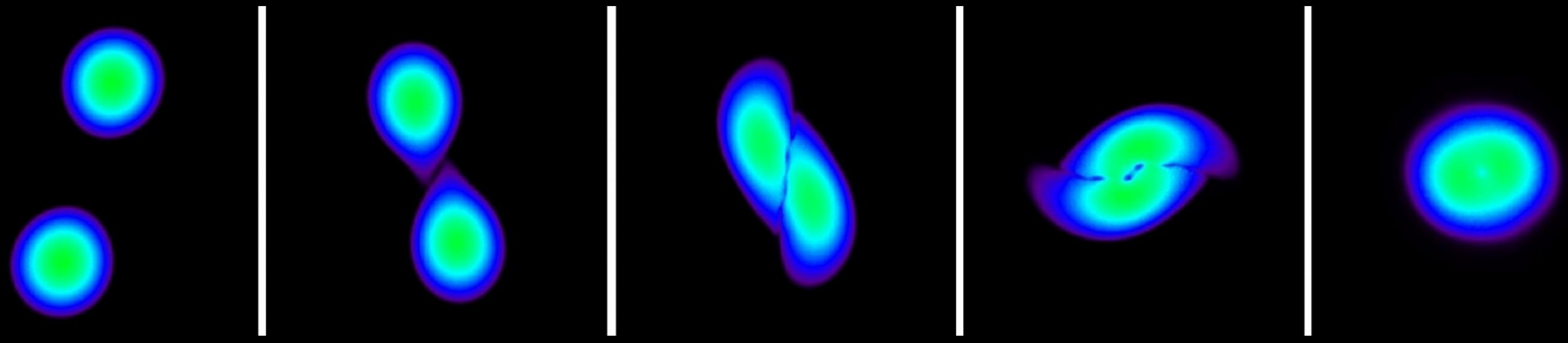

# Description of tidal effects during inspiral

- Tidal field $E_{ij}$ of on star induces change of quadrupole moment $Q_{ij}$ of other component
- Changed quadrupole moment affects GW signal, especially phase
- Strength of induced quadrupole moment depends on NS structure / EoS:

$$Q_{ij} = -\lambda(M)\, E_{ij} \qquad \lambda(M) = \frac{2}{3} k_2(M) R^5$$

- Tidal deformability depends on radius (clear – smaller stars are harder to deform) and "Love number" $k_2$ (~"TOV" properties)
- $k_2$ also depends on EoS and mass

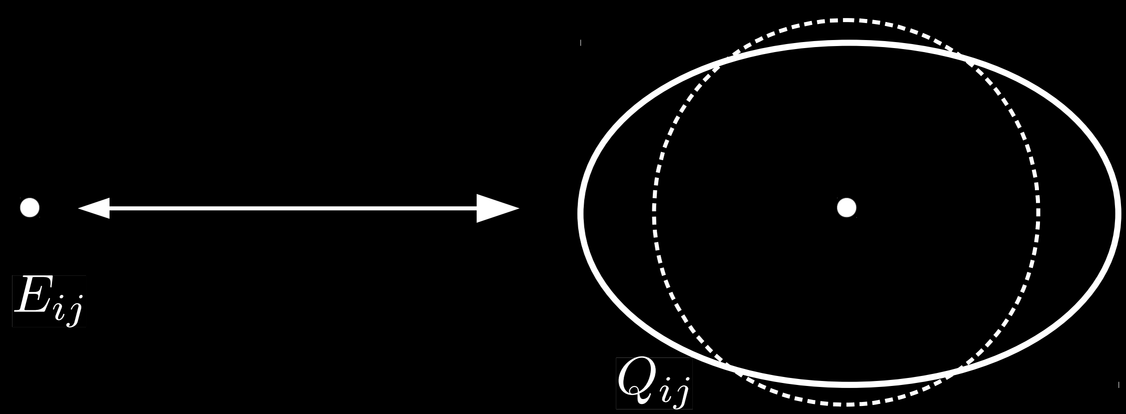

# Tidal effects during the inspiral

- Tidal deformability enters waveform description $\lambda(M) = \frac{2}{3} k_2(M) R^5$

  (hence tidal deformability is measured in GW event)

- Challenge: describe waveform accurately and effectively to construct template bank for detection (match with numerical simulation): PN expansion, effective one-body models (EOB)

- Compute tidal deformability for given EoS and mass:

  - radius via TOV (easy)

  - Love number $k_2$ can be computed in a similar manner

  → essentially an extended TOV system, i.e. system of ordinary differential equations that can be solved as initial value problem

# Love number

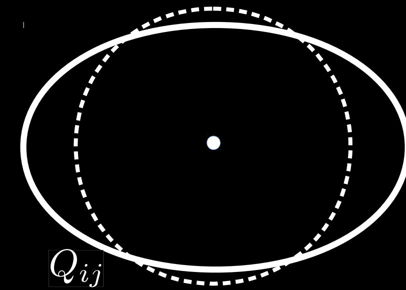


l=2 metric perturbation of spherical star
→ encoded in H(r), K(r) (depend only on r !!!)

$$\begin{aligned} ds^2 &= -e^{2\Phi(r)}\left[1 + H(r)Y_{20}(\theta,\varphi)\right]dt^2 \\ &\quad + e^{2\Lambda(r)}\left[1 - H(r)Y_{20}(\theta,\varphi)\right]dr^2 \\ &\quad + r^2\left[1 - K(r)Y_{20}(\theta,\varphi)\right]\left(d\theta^2 + \sin^2\theta d\varphi^2\right) \end{aligned}$$

Solve standard TOV system:

$$\begin{aligned} e^{2\Lambda} &= \left(1 - \frac{2m_r}{r}\right)^{-1}, \\ \frac{d\Phi}{dr} &= -\frac{1}{\epsilon + p}\frac{dp}{dr}, \\ \frac{dp}{dr} &= -(\epsilon + p)\frac{m_r + 4\pi r^3 p}{r(r - 2m_r)}, \\ \frac{dm_r}{dr} &= 4\pi r^2 \epsilon. \end{aligned}$$

Lecture by Stergioulas

And integrate in parallel:

$$\begin{aligned} \frac{dH}{dr} &= \beta \\ \frac{d\beta}{dr} &= 2\left(1 - 2\frac{m_r}{r}\right)^{-1} H \left\{-2\pi\left[5\epsilon + 9p + f(\epsilon + p)\right]\right. \\ &\quad \left. + \frac{3}{r^2} + 2\left(1 - 2\frac{m_r}{r}\right)^{-1}\left(\frac{m_r}{r^2} + 4\pi r p\right)^2\right\} \\ &\quad + \frac{2\beta}{r}\left(1 - 2\frac{m_r}{r}\right)^{-1}\left\{-1 + \frac{m_r}{r} + 2\pi r^2(\epsilon - p)\right\} \end{aligned}$$

→ system of ordinary differential equations that can be solved as initial value problem

Hinderer et al. 2010

# Love number and tidal deformability

- Love number given by:

$$
\begin{aligned}
k_2 = \; & \frac{8C^5}{5}(1-2C)^2[2+2C(y-1)-y] \\
& \times\Big\{2C[6-3y+3C(5y-8)] \\
& \quad + 4C^3[13-11y+C(3y-2)+2C^2(1+y)] \\
& \quad + 3(1-2C)^2[2-y+2C(y-1)]\ln(1-2C)\Big\}^{-1},
\end{aligned}
$$

with $y = \frac{R\,\beta(R)}{H(R)}$

Compactness C, radius R
Mass m

$C = m/R$

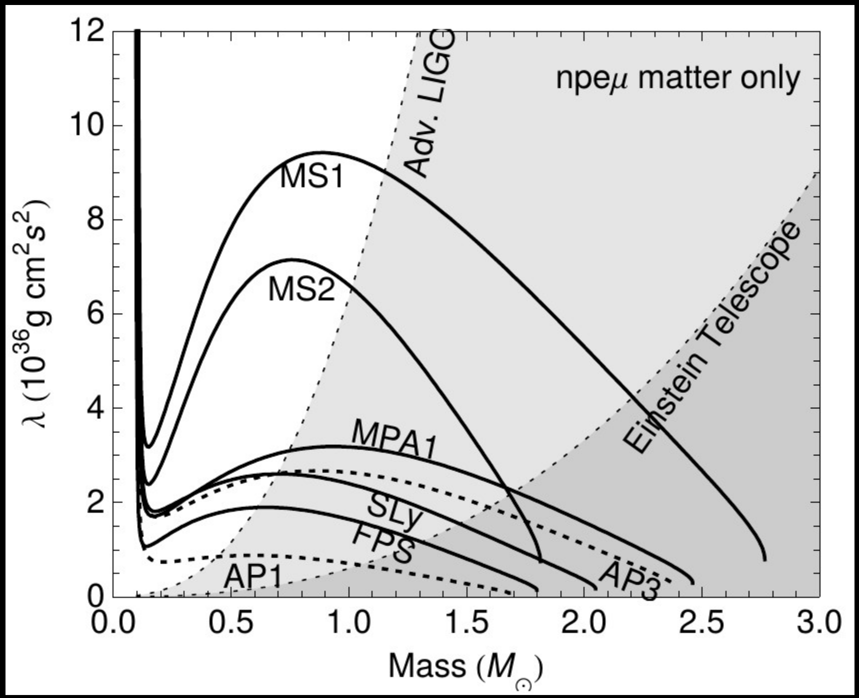


$$\lambda(M) = \frac{2}{3}k_2(M)R(M)^5$$

→ Larger/lighter stars have larger tidal defromability

→ Stiffer EoS have have deformability

→ discern different EoSs (for known mass)

Hinderer et al. 2010

# Inspiral

- Orbital phase evolution affected by NS radius (precisely tidal deformability) – only during last orbits before merging
- Difference in phase between NS merger and point-particle inspiral:

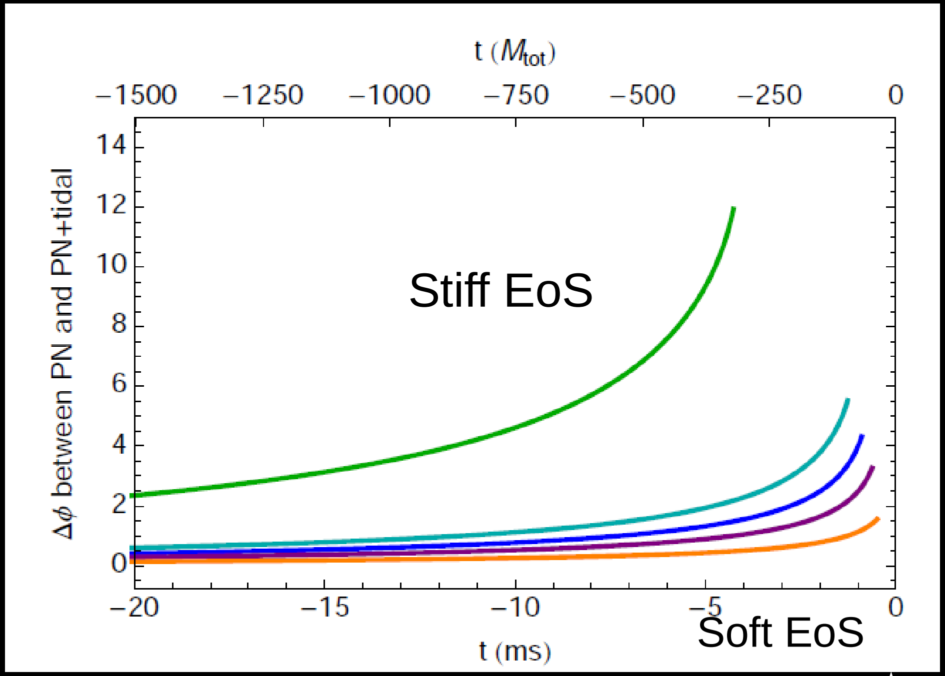


EoS impact measured by tidal deformability

$$\Lambda(M) = \frac{2}{3} k_2(M) \left( \frac{c^2 R}{G M} \right)^5$$

e.g. Read et al. 2013

Merger time of point particle

Challenge: construct faithful templates for data analysis

# Measurement

- Lambda < ~800

  → Means that very stiff EoSs are excluded

- Recall uncertainties in mass measurements (only Mchirp accurate)
- BUT: systematic errors not included !!!

  → ongoing research

- Better constraints expected in future as sensitivity increases

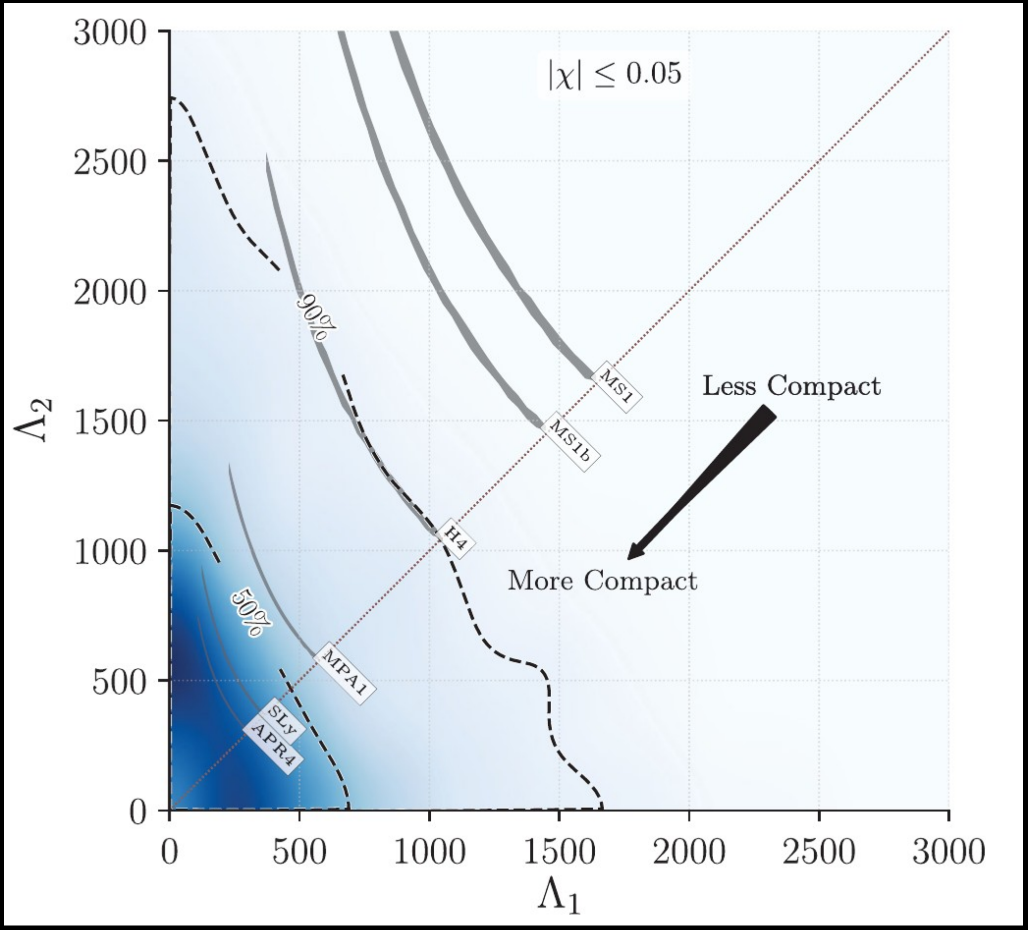


$$\tilde{\Lambda} = \frac{16}{13}\frac{(m_1 + 12m_2)m_1^4\Lambda_1 + (m_2 + 12m_1)m_2^4\Lambda_2}{(m_1+m_2)^5}$$

Abbott et al. 2017

- Tidal deformability vs. radius

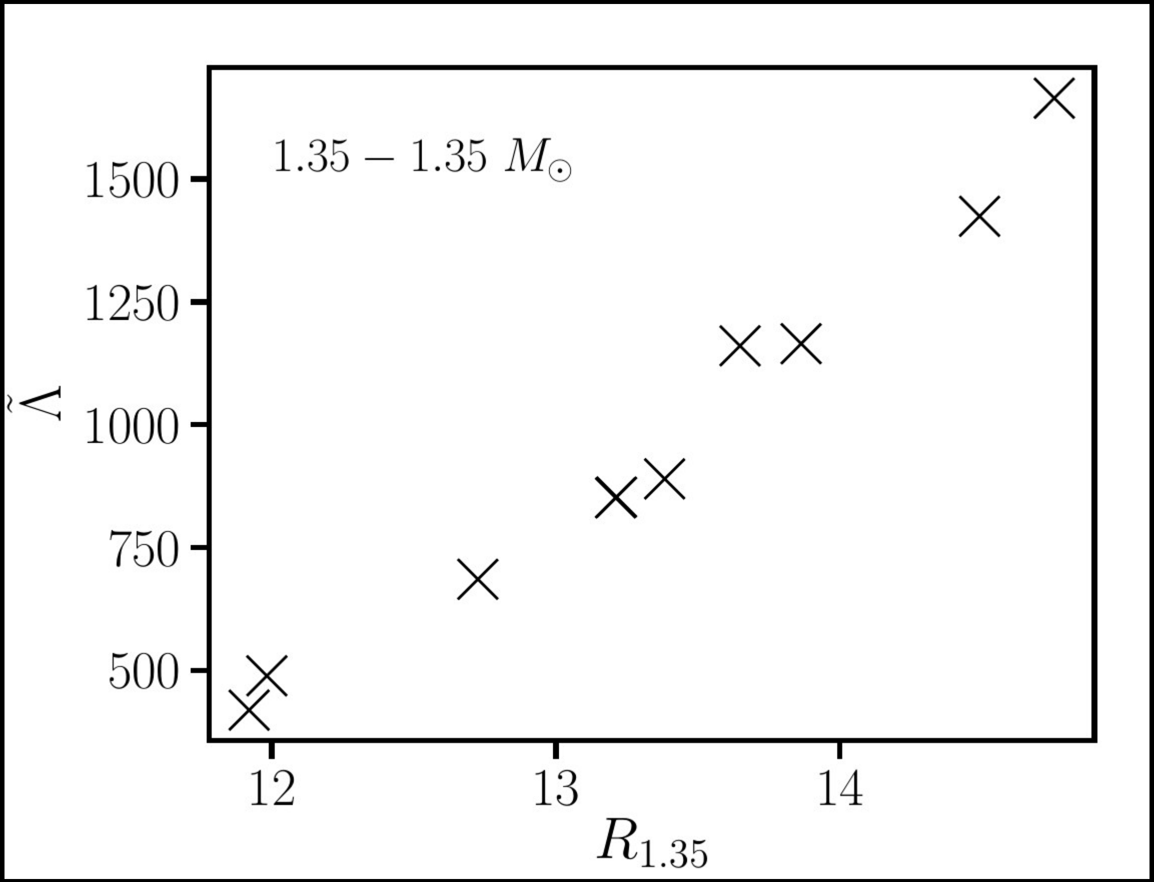

# Postmerger oscillations

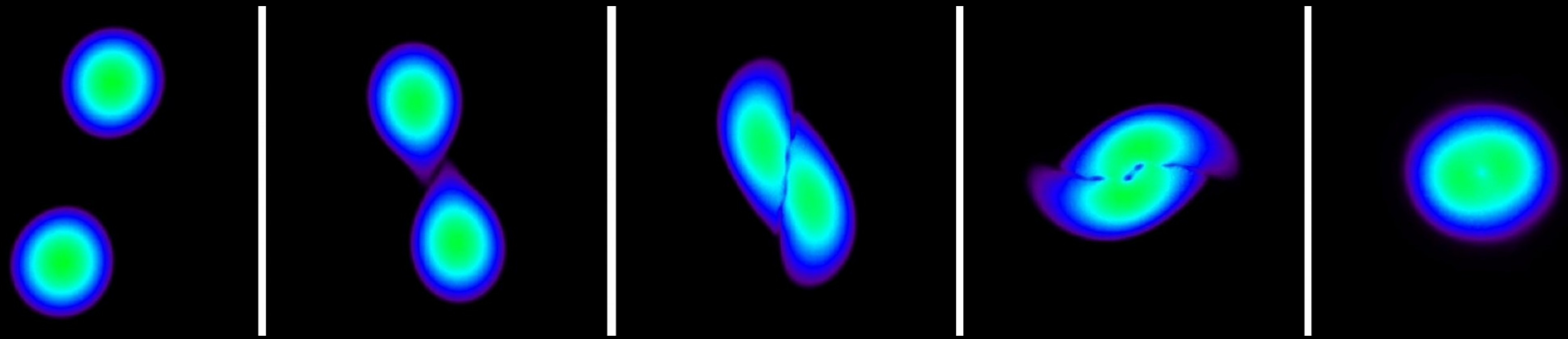

Complementary to inspiral,

# Simulation: 1.35+1.35 $M_{sun}$

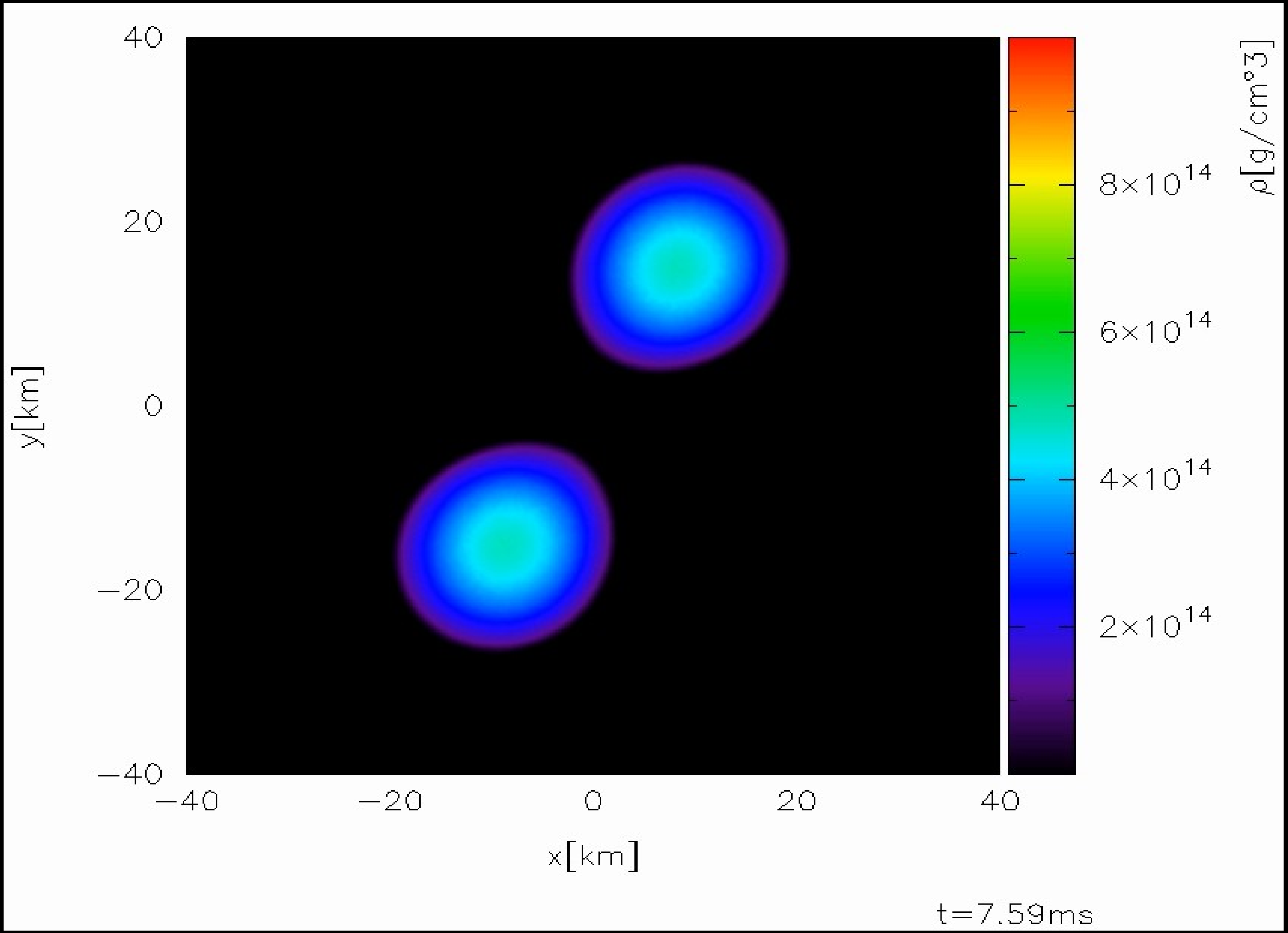


Density evolution in equatorial plane, Shen EoS

Relativistic smooth particle hydrodynamics, conformally flat spatial metric, microphsyical temperature-dependent EoS

1.35-1.35 Msun, Shen EoS

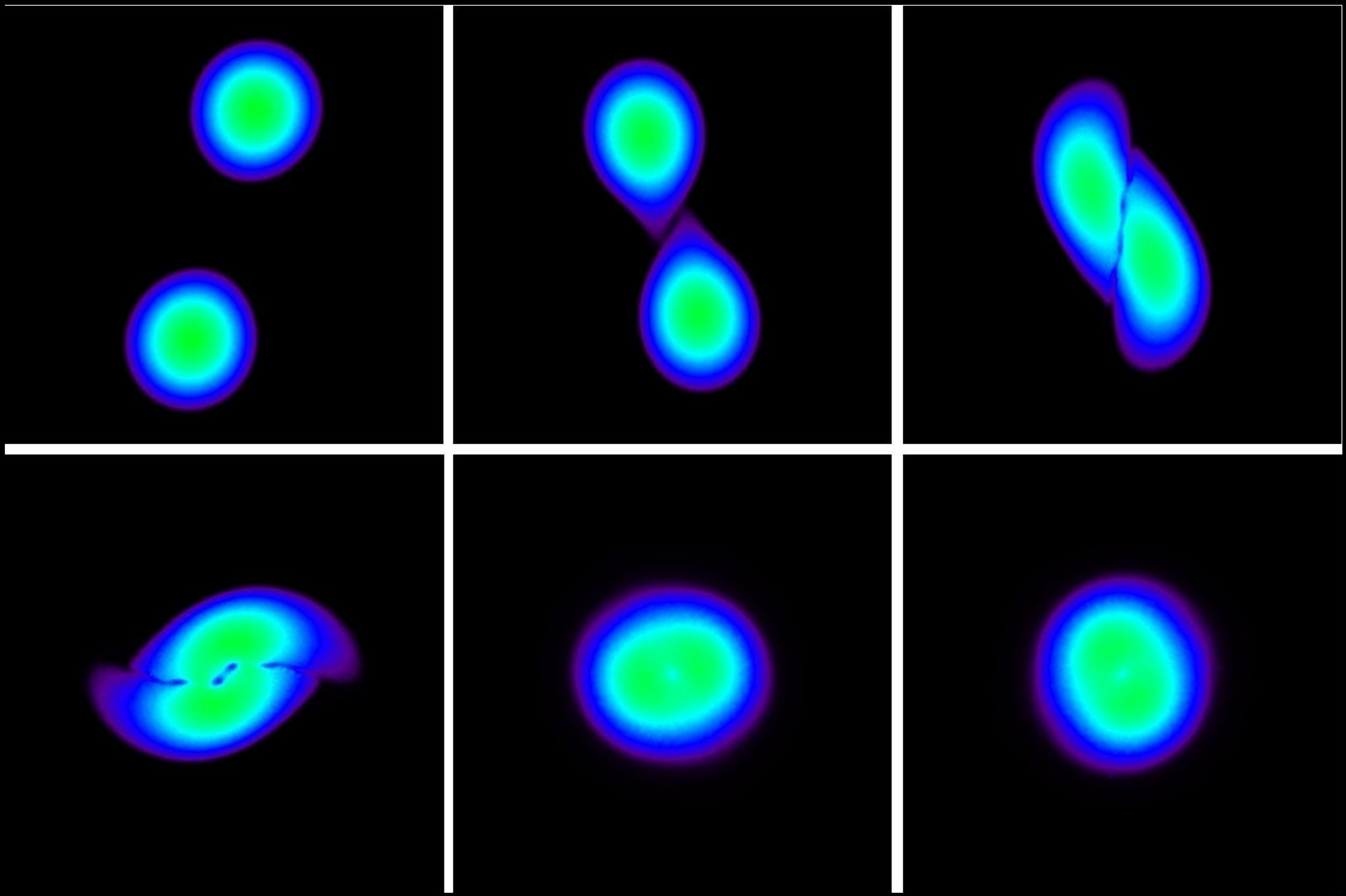

Relativistic smooth particle hydrodynamics, conformally flat spatial metric, microphsyical temperature-dependent EoS

# Postmerger

1.35-1.35 $M_{sun}$ , 20 Mpc

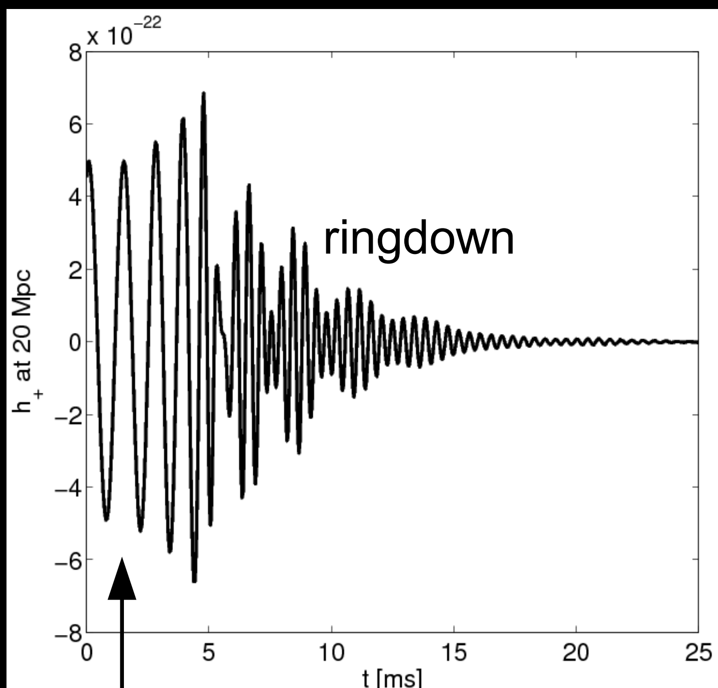


inspiral

Earlier inspiral

EoS

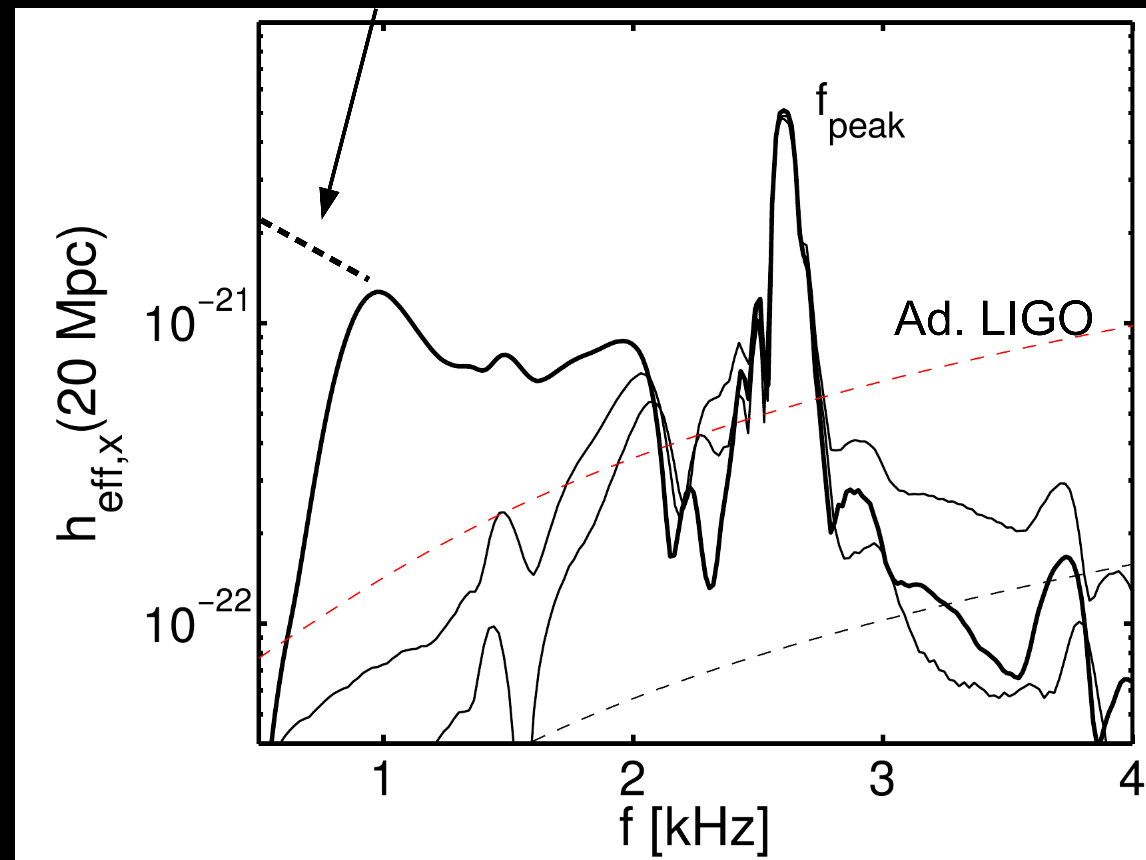


Dominant postmerger oscillation frequency $f_{peak}$

Very characteristic (robust feature in all models)

Every data point a single simulation of a 1.35-1.35 $M_{sun}$ binary

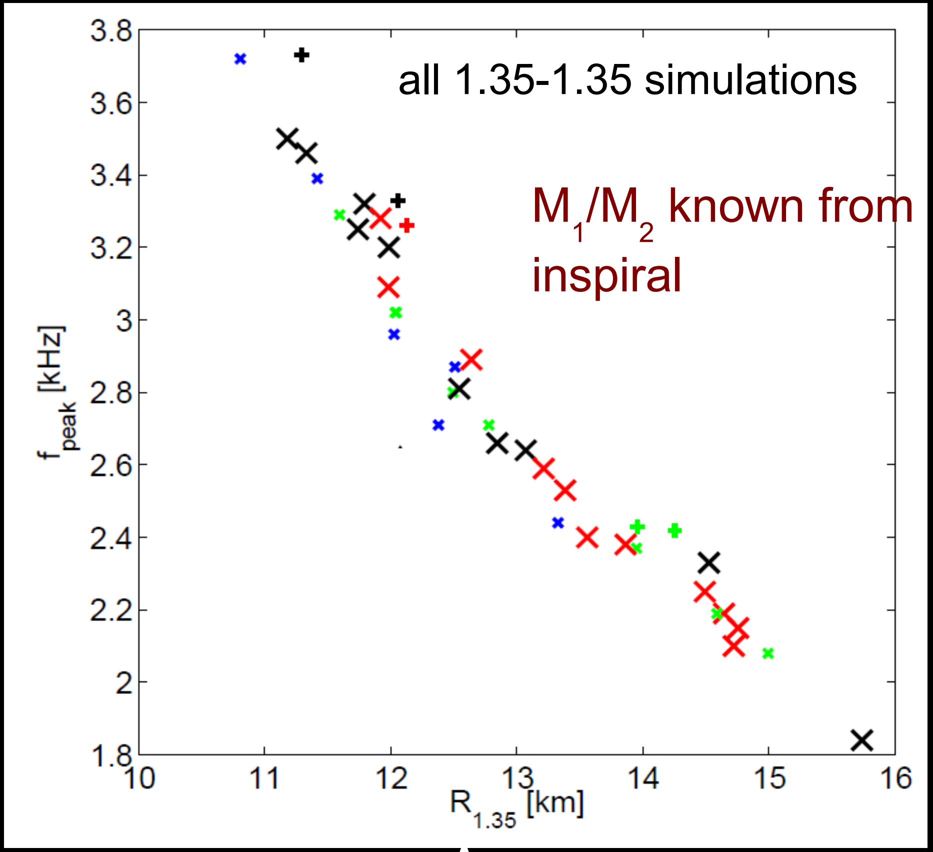


Bauswein et al. 2012

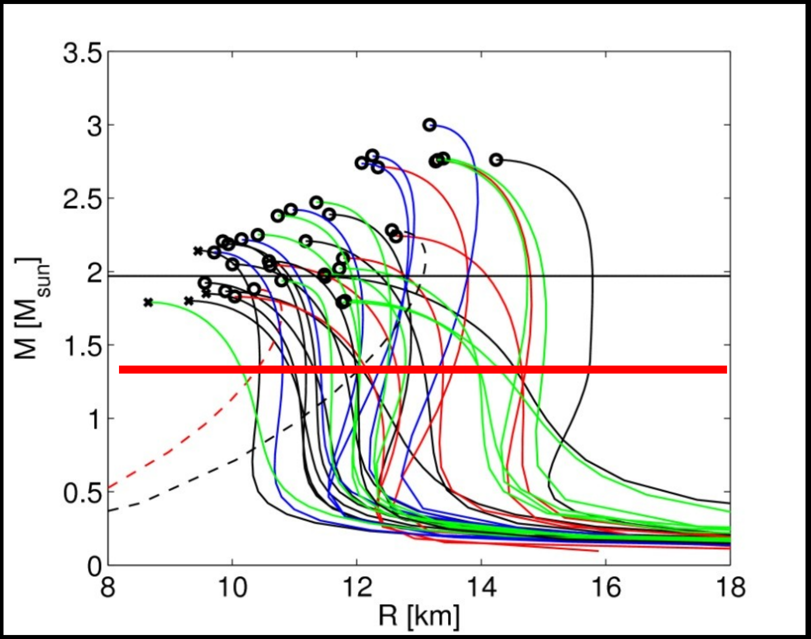


characterize EoS by radius of nonrotating NS with 1.35 $M_{sun}$

Pure TOV property => Radius measurement via $f_{peak}$

→ Empirical relation between GW frequency and NS radius ( = our EoS parameter)

Important: Simulations for the same binary mass, but with varied EoS

Recall that total mass can be measured quite accurately

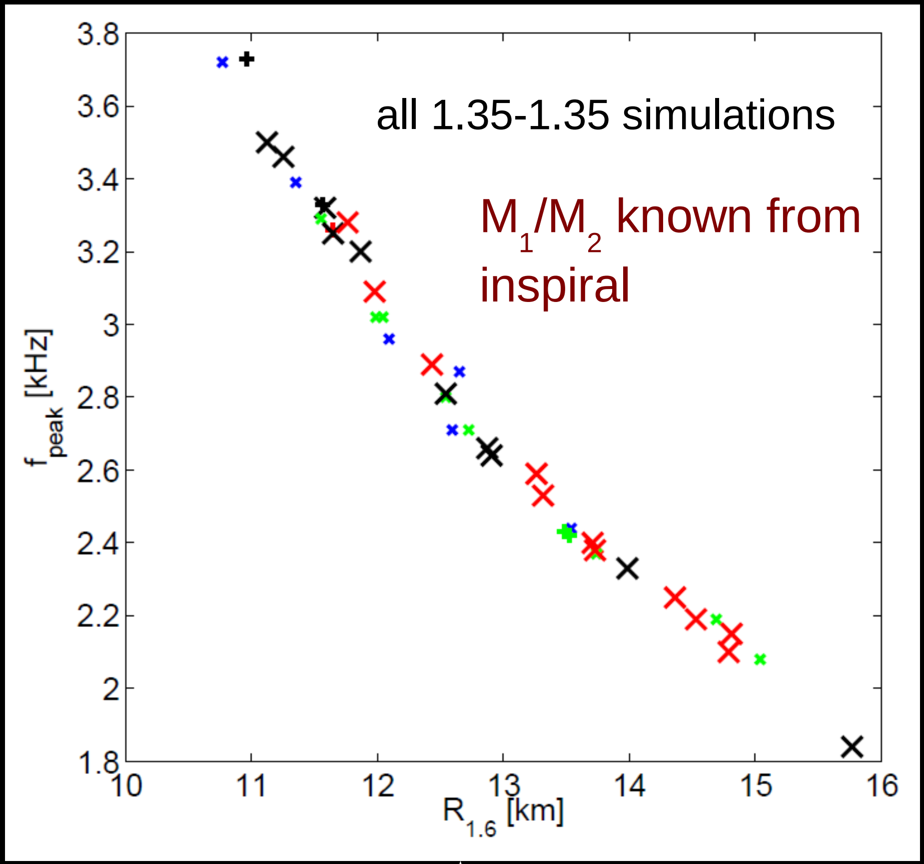


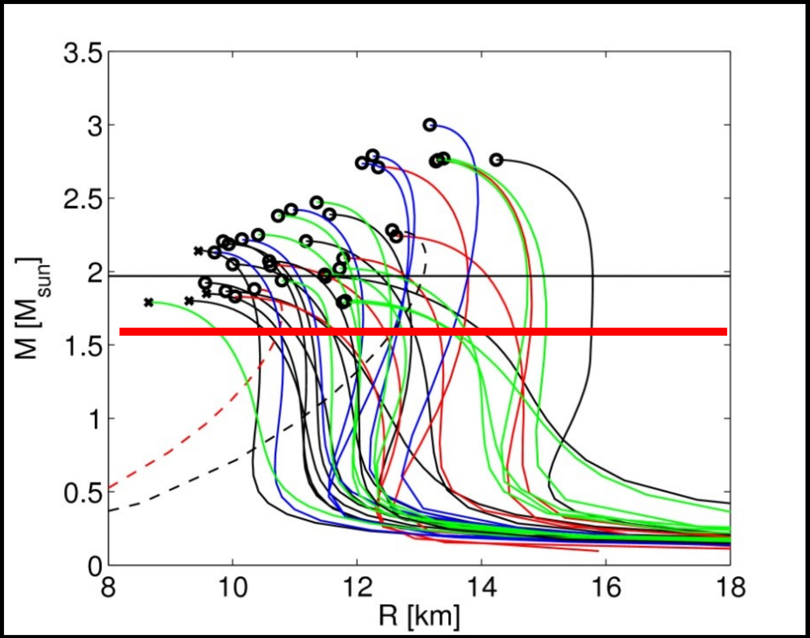


characterize EoS by radius of nonrotating NS with 1.6 $M_{sun}$

Bauswein et al. 2012

Pure TOV/EoS property => Radius measurement via $f_{peak}$

Fit: $R(1.6\ M_\odot) = 1.1\, f_{GW}^2 - 8.6\, f_{GW} + 28.$

Important: Simulations for the same binary mass, just with varied EoS

# Binary mass variations

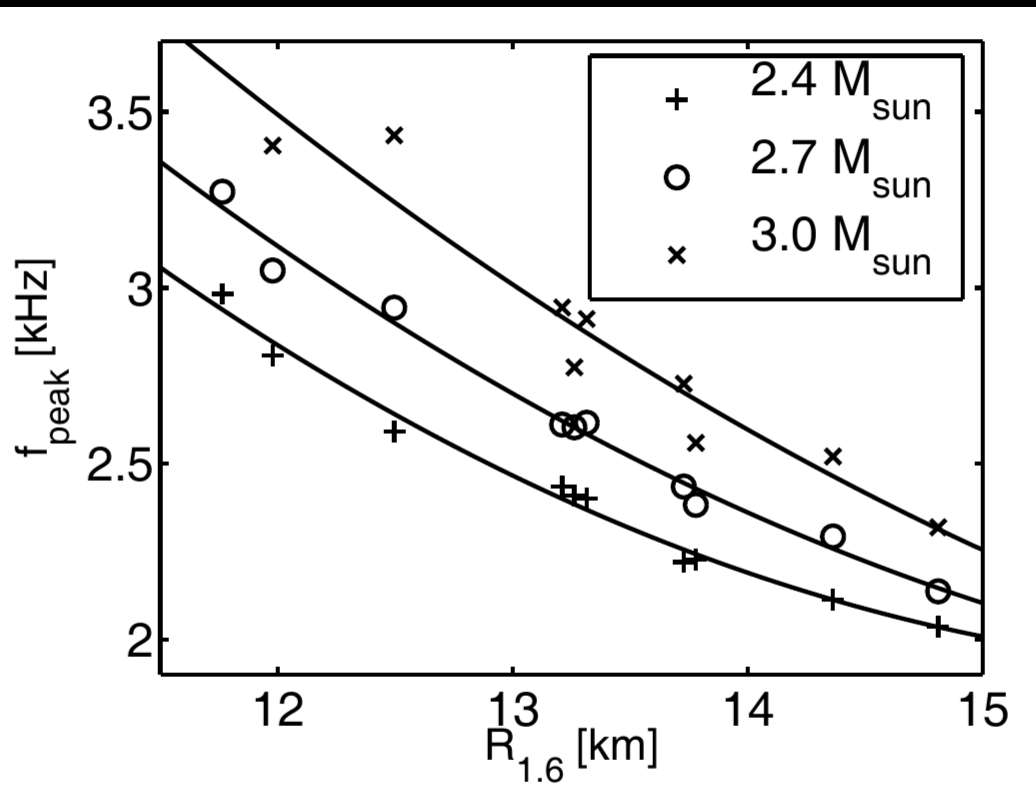


Different total binary masses (symmetric)

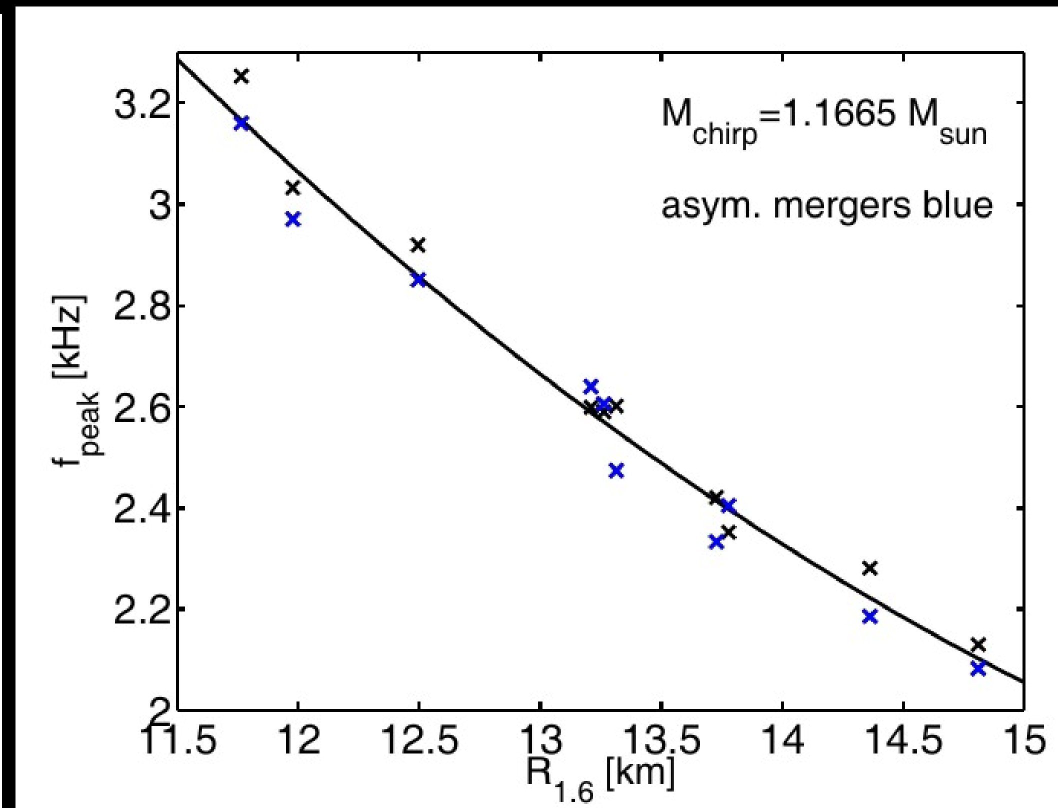


Fixed chirp mass (asymmertic 1.2-1.5 $M_{sun}$ binaries and symmetric 1.34-1.34 $M_{sun}$ binaries)

Bauswein et al. 2012, 2016

# Strategy for radius measurements

- Measure binary masses from inspiral
- Construct $f_{peak}$ – R relation for this fixed binary masses and (optimally) chosen R
- Measure $f_{peak}$ from postmerger GW signal
- Obtain radius by inverting $f_{peak}$ – R relation
- (possibly restrict to fixed mass ratios if mergers with high asymmetry are measured)

- Final error of radius measurement:

  - accuracy of $f_{peak}$ measurement (see Clark et al. 2014, Clark et al. 2016)

  - maximum scatter in f-R relation (important to consider very large sample of EoSs)

  - systematic error in f-R relation

# GW data analysis

Searches performed for GW170817, but only upper limits -  not surprising

→ but very promising at design sensitivity

→ data analysis – ongoing research

# Data analysis – prove of principle

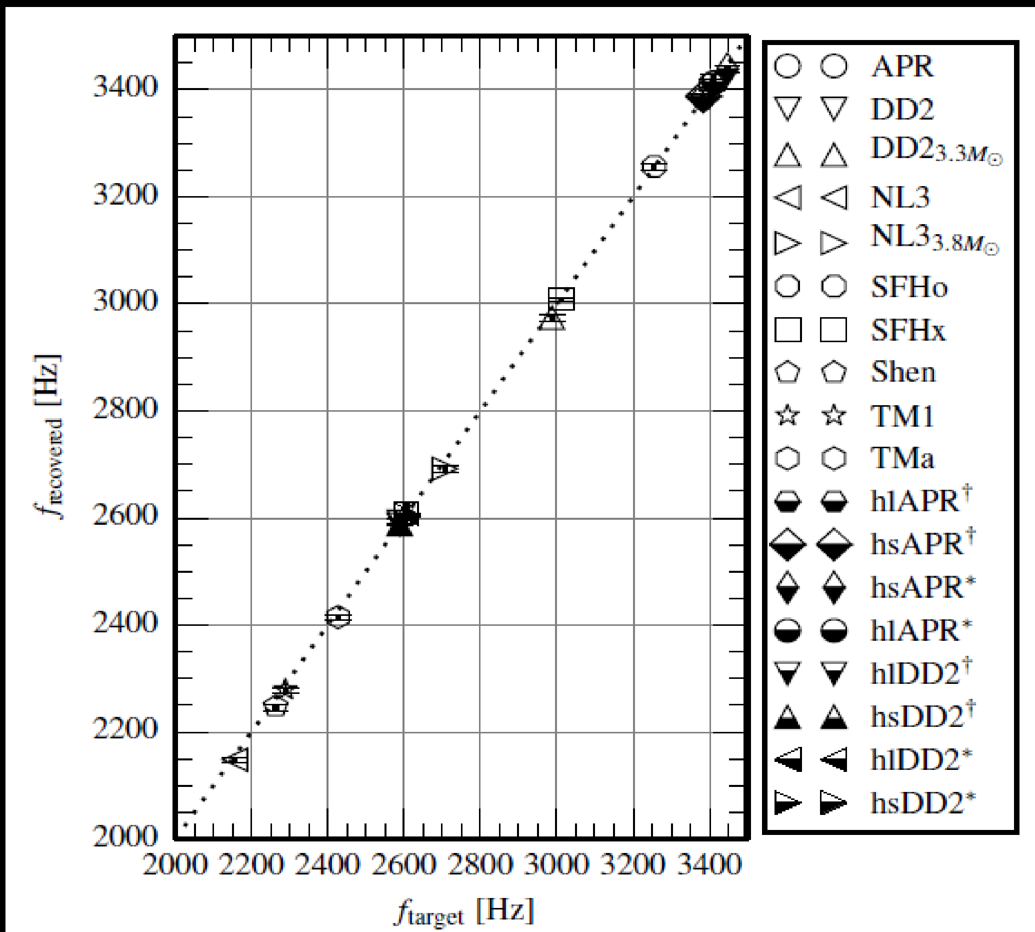


Model waveforms hidden in rescaled LIGO noise

Peak frequency recovered with burst search analysis

Error ~ 10 Hz

For signals within ~10-25 Mpc

=> for near-by event radius measurable with high precision (~0.01-1/yr)

Proof-of-principle study
→ improvements likely

Clark et al. 2014

# Data analysis

- Principal Component analysis

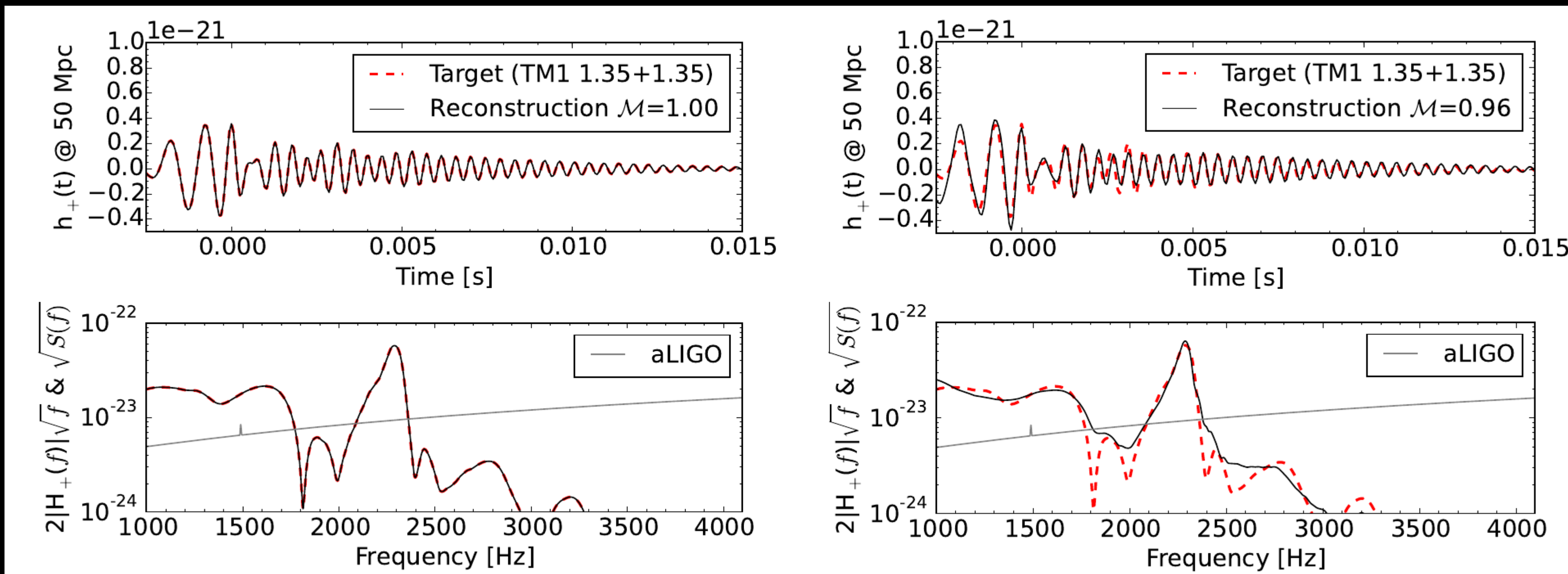


Clark et al. 2016

Excluding recovered waveform from catalogue

| Instrument | $\mathrm{SNR}_{\mathrm{full}}$ | $D_{\mathrm{hor}}$ [Mpc] | $\dot{N}_{\mathrm{det}}$ [$\mathrm{year}^{-1}$] |
|---|---|---|---|
| aLIGO | $2.99^{3.86}_{2.37}$ | $29.89^{38.57}_{23.76}$ | $0.01^{0.03}_{0.01}$ |
| A+ | $7.89^{10.16}_{6.25}$ | $78.89^{101.67}_{62.52}$ | $0.13^{0.20}_{0.10}$ |
| LV | $14.06^{18.13}_{11.16}$ | $140.56^{181.29}_{111.60}$ | $0.41^{0.88}_{0.21}$ |
| ET-D | $26.65^{34.28}_{20.81}$ | $266.52^{342.80}_{208.06}$ | $2.81^{5.98}_{1.33}$ |
| CE | $41.50^{53.52}_{32.99}$ | $414.62^{535.221}_{329.88}$ | $10.59^{22.78}_{5.33}$ |

Outdated!!!

→ possible at Ad. LIGO's design sensitivity !

# Model-agnostic data analysis

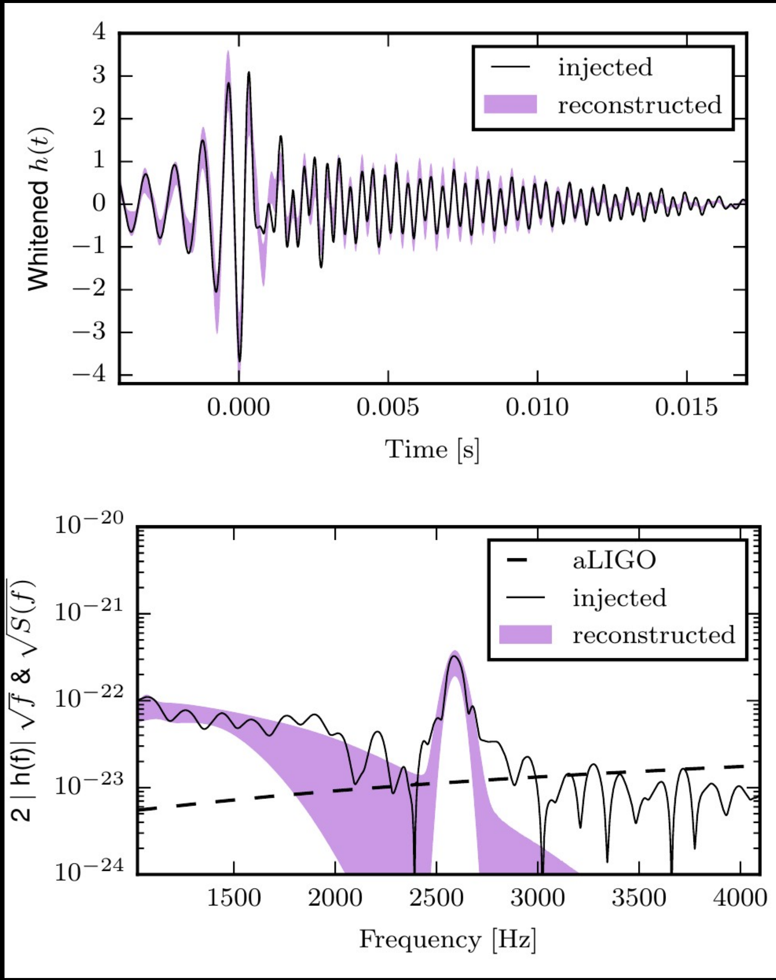


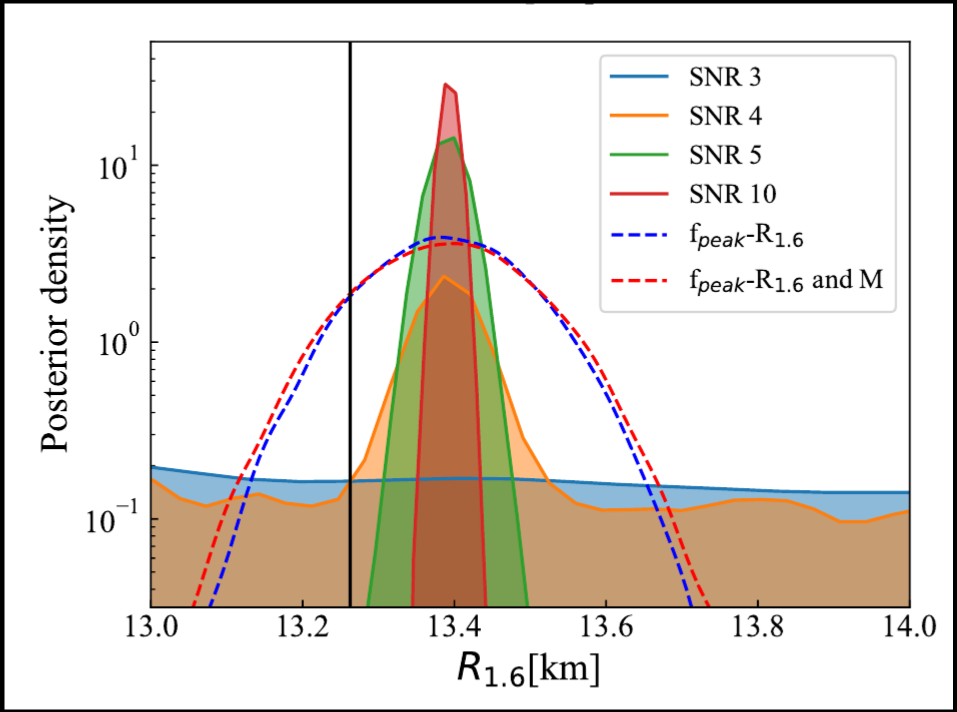


Chatziioannou et al. (2017)

# Background: physical mechanisms

# Dominant oscillation frequency

- Robust feature, which occurs in all models (which don't collapse promptly to BH)
- Fundamental quadrupolar fluid mode of the remnant

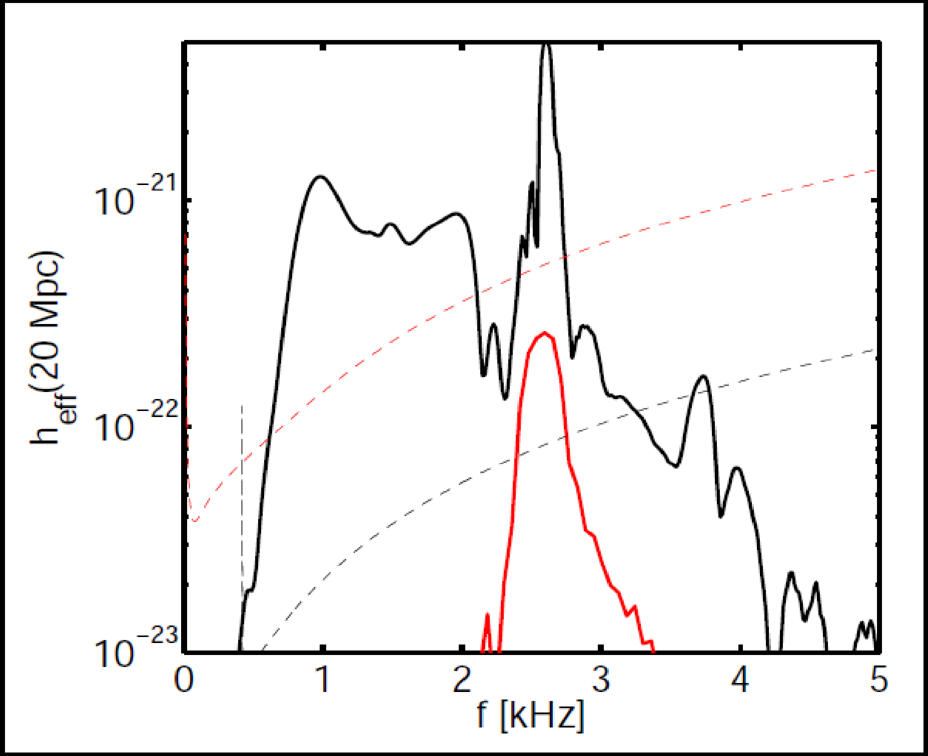


Re-excitation of f-mode (l=|m|=2) in late-time remnant (Bauswein et al. 2016)

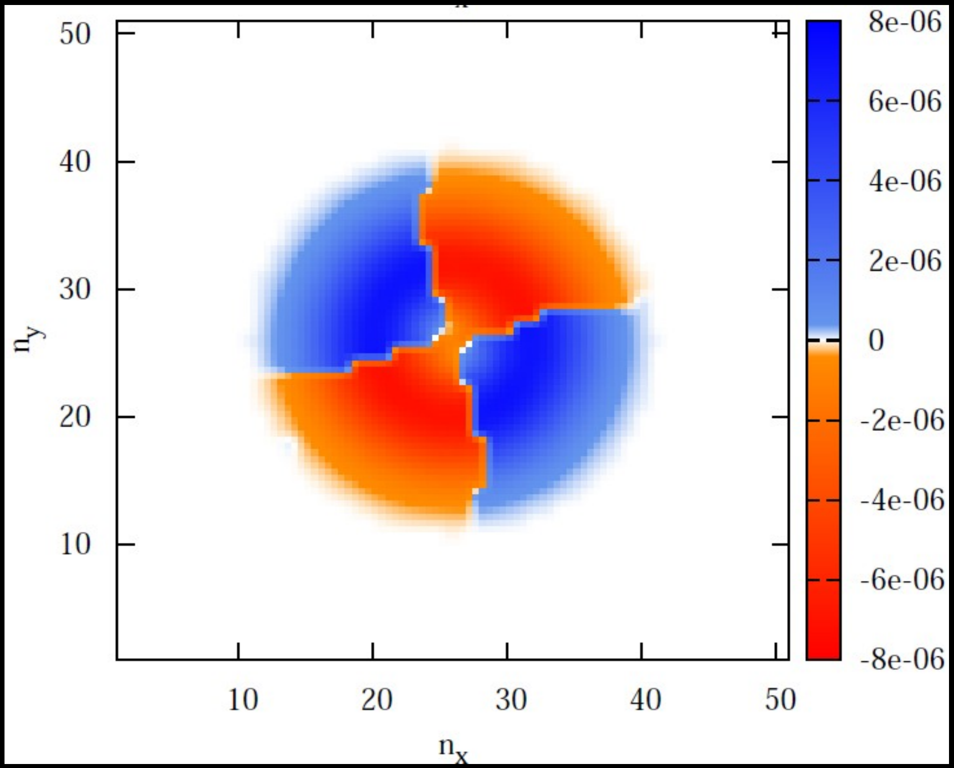


Mode analysis at $f=f_{peak}$
Stergioulas et al. 2011

# Secondary GW features

- A lot of substructure in the GW spectrum, especially subdominant peaks at lower frequencies are observationally relevant
- To some extent a NS merger remnant is just a big, rotating, oscillating NS → but which modes? → further effects?
- Two secondary features identified:

  - radial mode (no GW emission) couples to quadrupole mode → emission at $f_{peak} \pm f_0$

  - tidal bulges form during merging and contribute for a few milliseconds
- Presence and strength of these features depends on EoS and binary masses → classification scheme of dynamics and GW spectra
- Similar relations for secondary frequencies (but harder to detect)

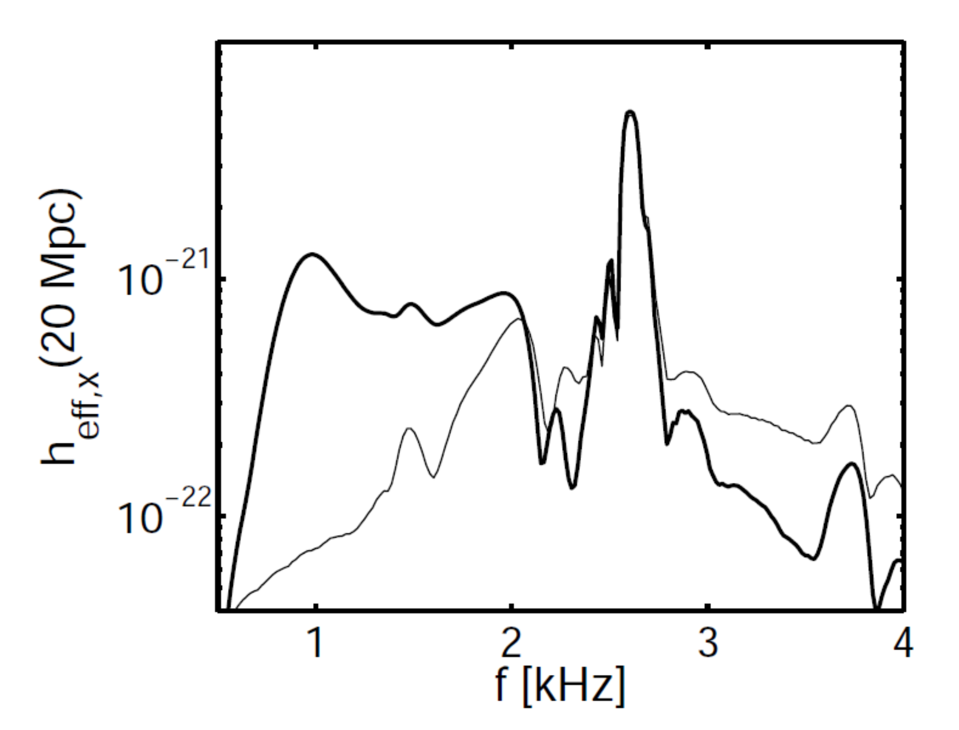


Bauswein et al. 2015

# Example: TM1 1.35-1.35 Msun, strong tidal bulges, weak radial oscillation (e.g. from analysis of lapse)

Clark et al. 2016

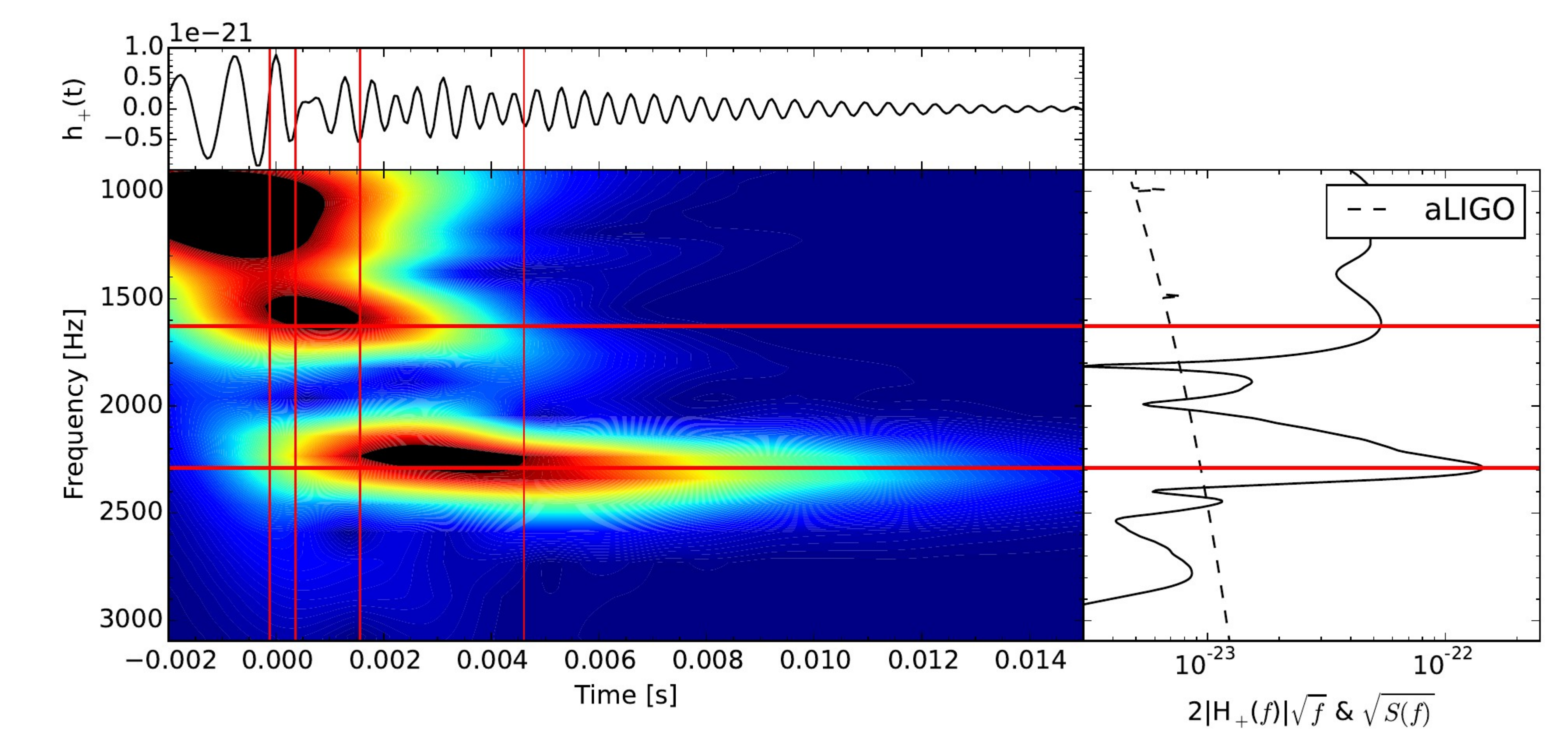


Note: different ideas about the origin of the peaks, e.g. Kastaun & Galeazzi 2015, Takami et al. 2014, 2015 propose a strongly varying instantaneous frequency that produces side peaks

# Collapse behavior

→ Radius constraints !

→ Constrain maximum mass

→ Conditions for short GRBs

→ Mass ejection

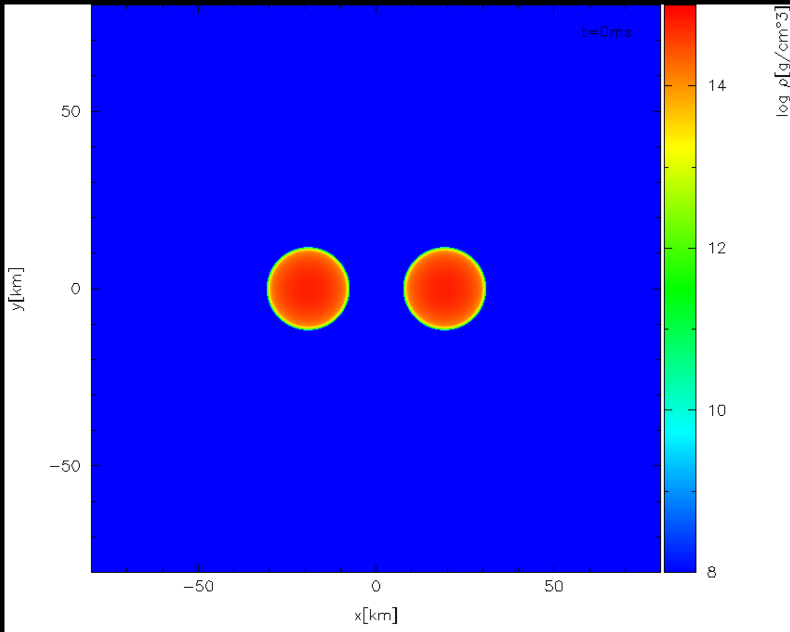


$M_{\rm tot} = 3.4\ M_\odot$

$M_{\rm tot} = 3.5\ M_\odot$

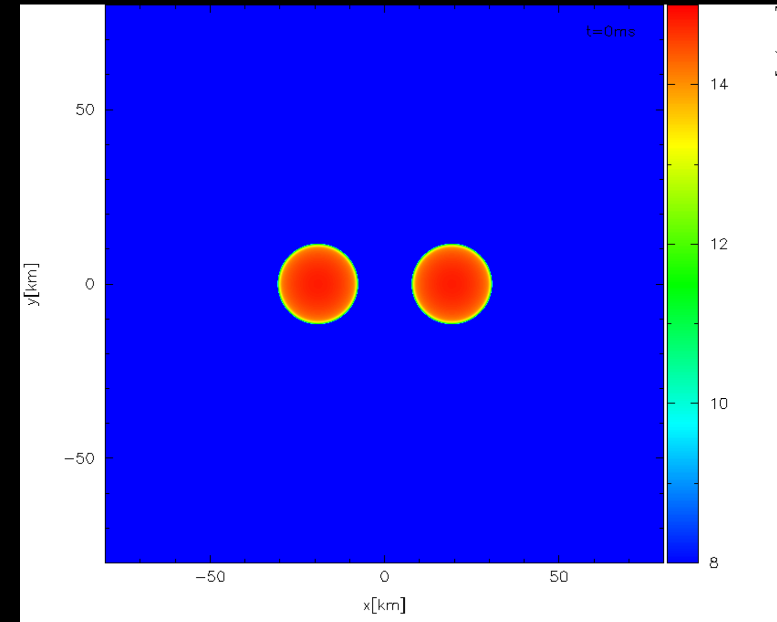


Shen EoS

# Collapse behavior: Prompt vs. delayed (/no) collapse

Relevant for:

EoS constraints through $M_{max}$ measurement

Conditions for short GRBs

Mass ejection

Electromagnetic counterparts powered by thermal emission

And NS radius constraints !!!

# Collapse behavior

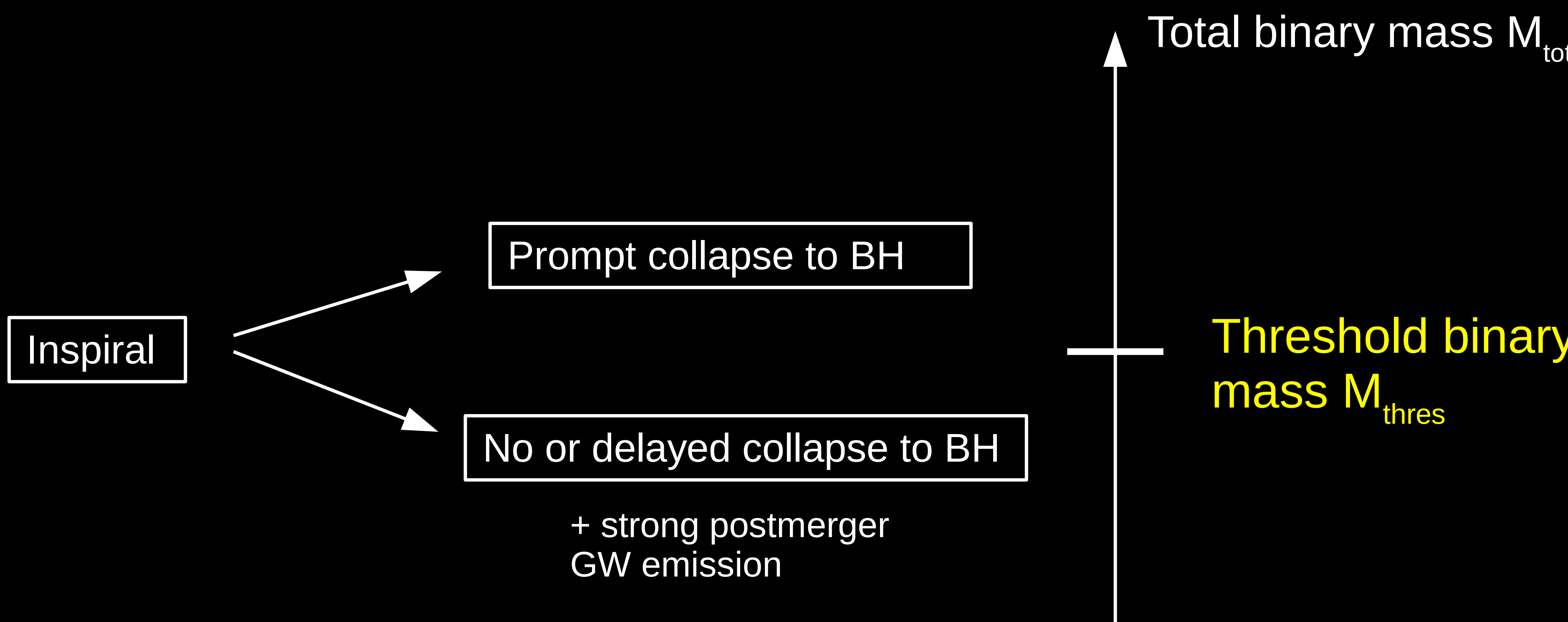


EoS dependent - somehow $M_{max}$ should play a role

→ … from observations we can determine $M_{max}$, $R_{max}$, $\rho_{max}$

# EoS constraints from GW170817

# Threshold binary mass

- Empirical relation from simulations with different Mtot and EoS
- To good accuracy:

$$M_{\mathrm{thres}} = \left( -3.6 \frac{G\, M_{\mathrm{max}}}{c^2\, R_{1.6}} + 2.38 \right)\, M_{\mathrm{max}}$$

$$M_{\mathrm{thres}} = \left( -3.38 \frac{G M_{\mathrm{max}}}{c^2 R_{\mathrm{max}}} + 2.43 \right) M_{\mathrm{max}}$$

- Both better than 0.1 Msun

# A simple but robust NS radius constraint from GW170817

- GW measurements reveal binary masses of merger very accurately:

  - total binary mass quite well: 2.74 Msun for GW170817

  - mass ratio harder to measure: 0.7-1.0 for GW170817

- High ejecta mass inferred from optical transient

  → provides strong support for a delayed/no collapse in GW170817

  → even asymmetric mergers that directly collapse do not produce such massive ejecta

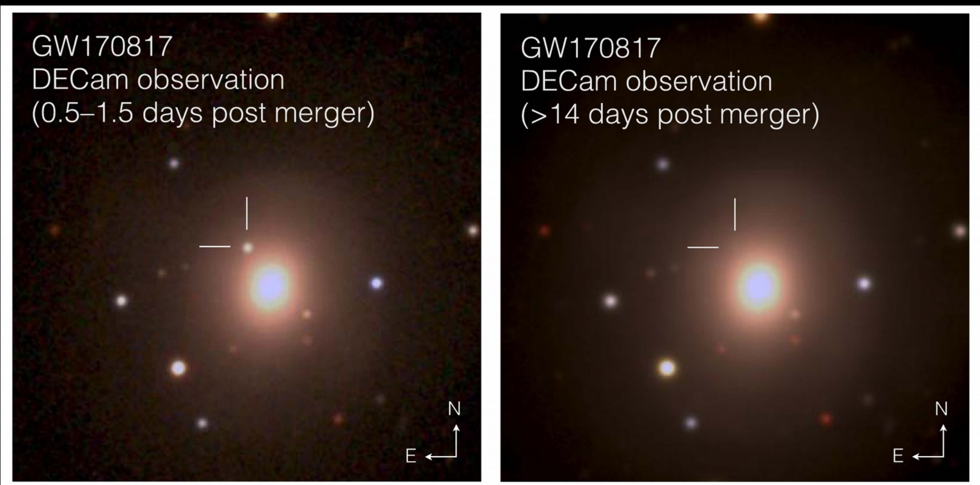


**Figure 1.** NGC4993 *grz* color composites ($1'.5 \times 1'.5$). Left: composite of detection images, including the discovery *z* image taken on 2017 August 18 00:05:23 UT and the g and r images taken 1 day later; the optical counterpart of GW170817 is at R.A., decl. =197.450374, −23.381495. Right: the same area two weeks later.

Soares-Santos et al 2017

- Ejecta masses depend on EoS and binary masses
- Note: high mass points already to soft EoS (tentatively/qualitatively)
- Prompt collapse leads to reduced ejecta mass
- Light curve depends on ejecta mass:

  → 0.02 - 0.05 Msun point to delayed collapse
- Note: here only dynamical ejecta

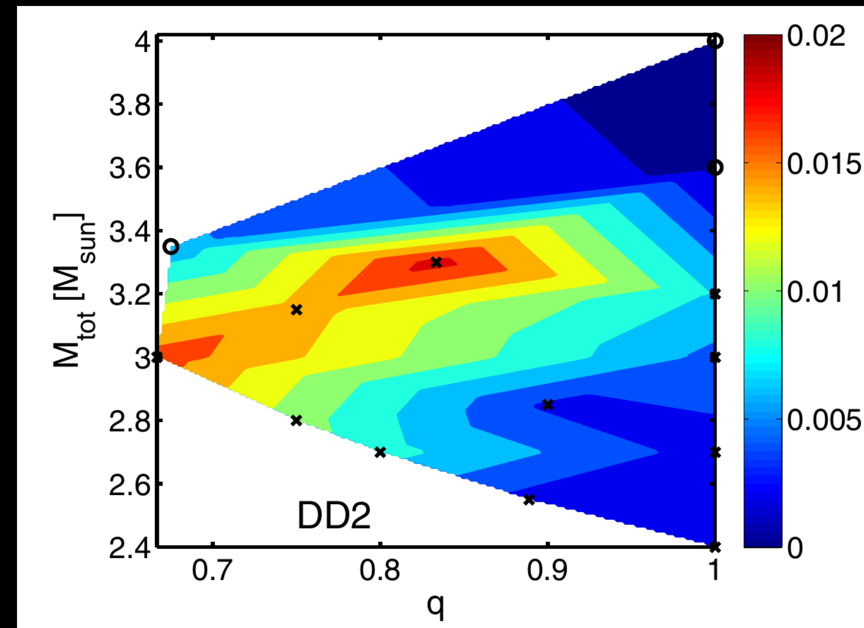


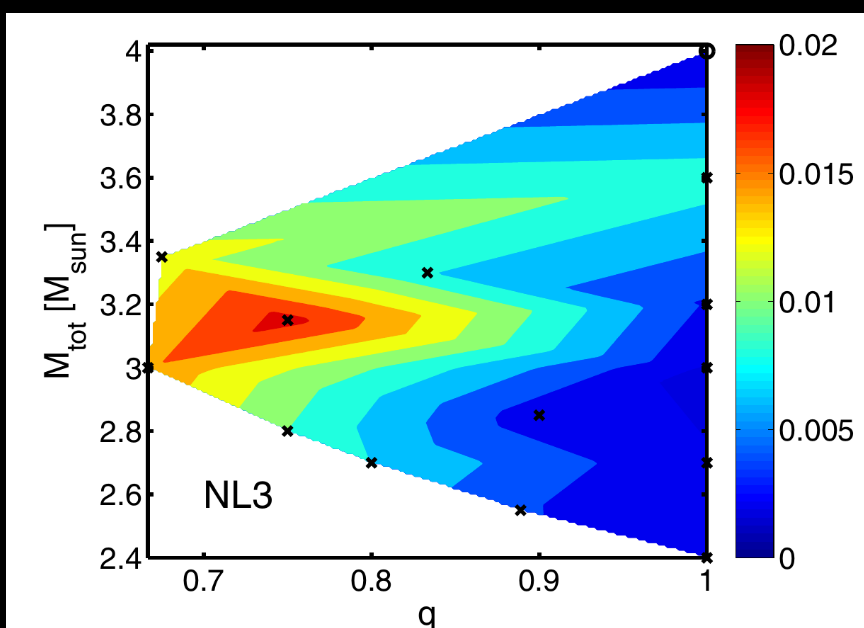


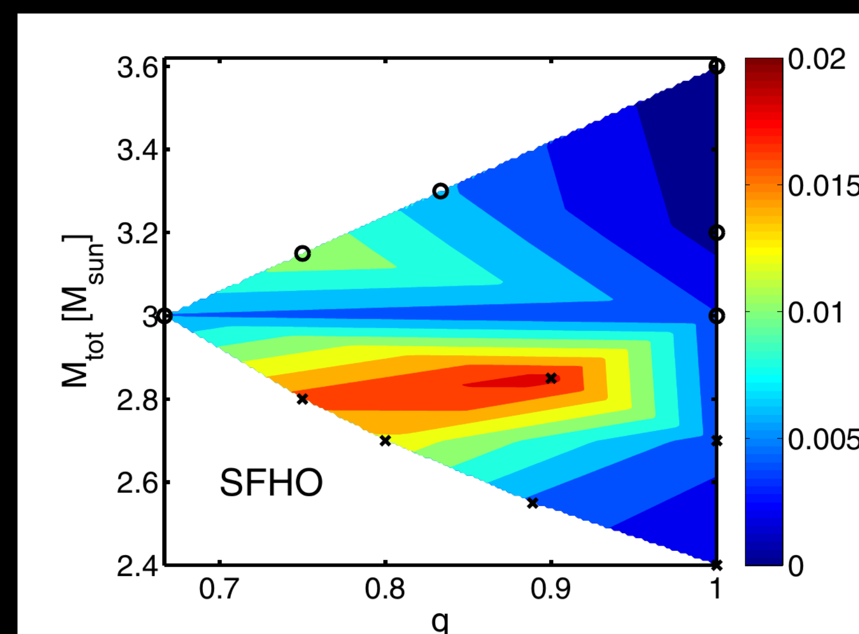


Bauswein et al. 2013

- GRB-like emission may be another argument for delayed collapse in GW170817

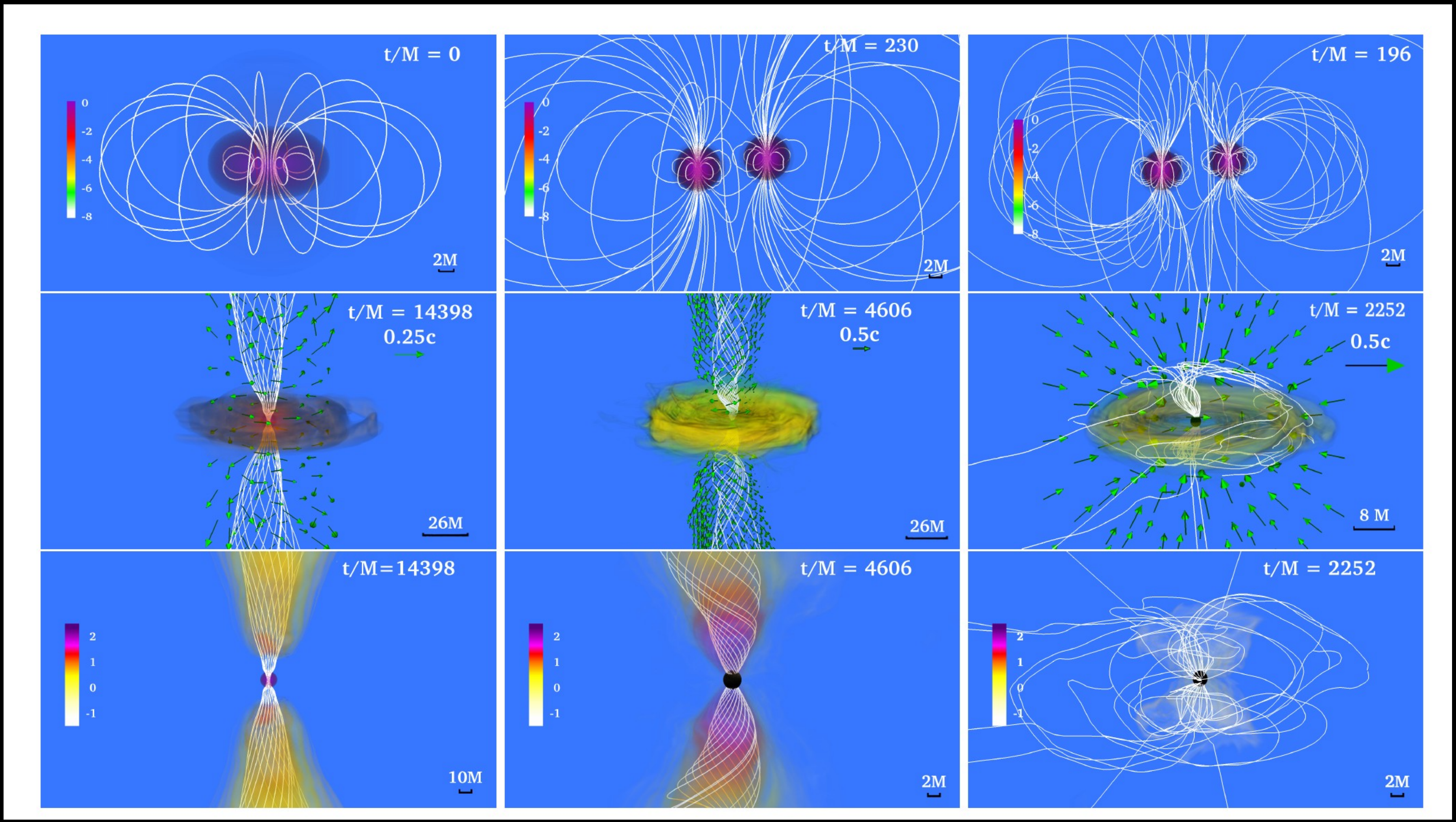


GRMHD simulations by Ruiz et al. 2017 suggest that delayed collapse required for jet formation

- If GW170817 was a delayed collapse:

$$M_{\mathrm{thres}} > M_{\mathrm{tot}}^{GW170817}$$

Recall: empirical relation for threshold binary mass for prompt collapse:

$$M_{\mathrm{thres}} = \left( -3.6 \frac{G\, M_{\mathrm{max}}}{c^2\, R_{1.6}} + 2.38 \right) M_{\mathrm{max}}$$

with Mmax, R16 unknown

Bauswein et al. 2017

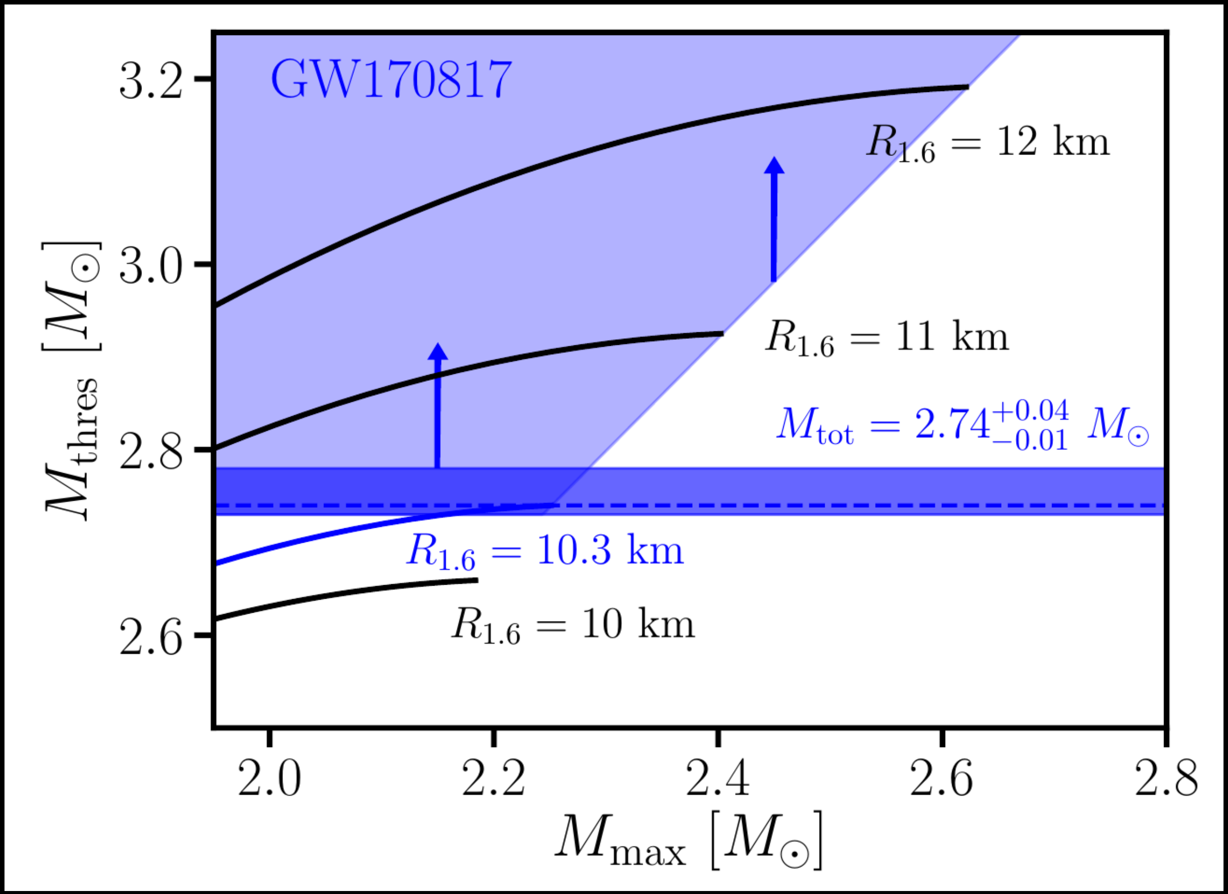


$$M_{\rm thres} = \left(-3.6 \frac{G\, M_{\rm max}}{c^2\, R_{1.6}} + 2.38\right)\, M_{\rm max}$$

+ causality → $M_{\rm thres} \geq 1.2 M_{\rm max}$

Bauswein et al. 2017

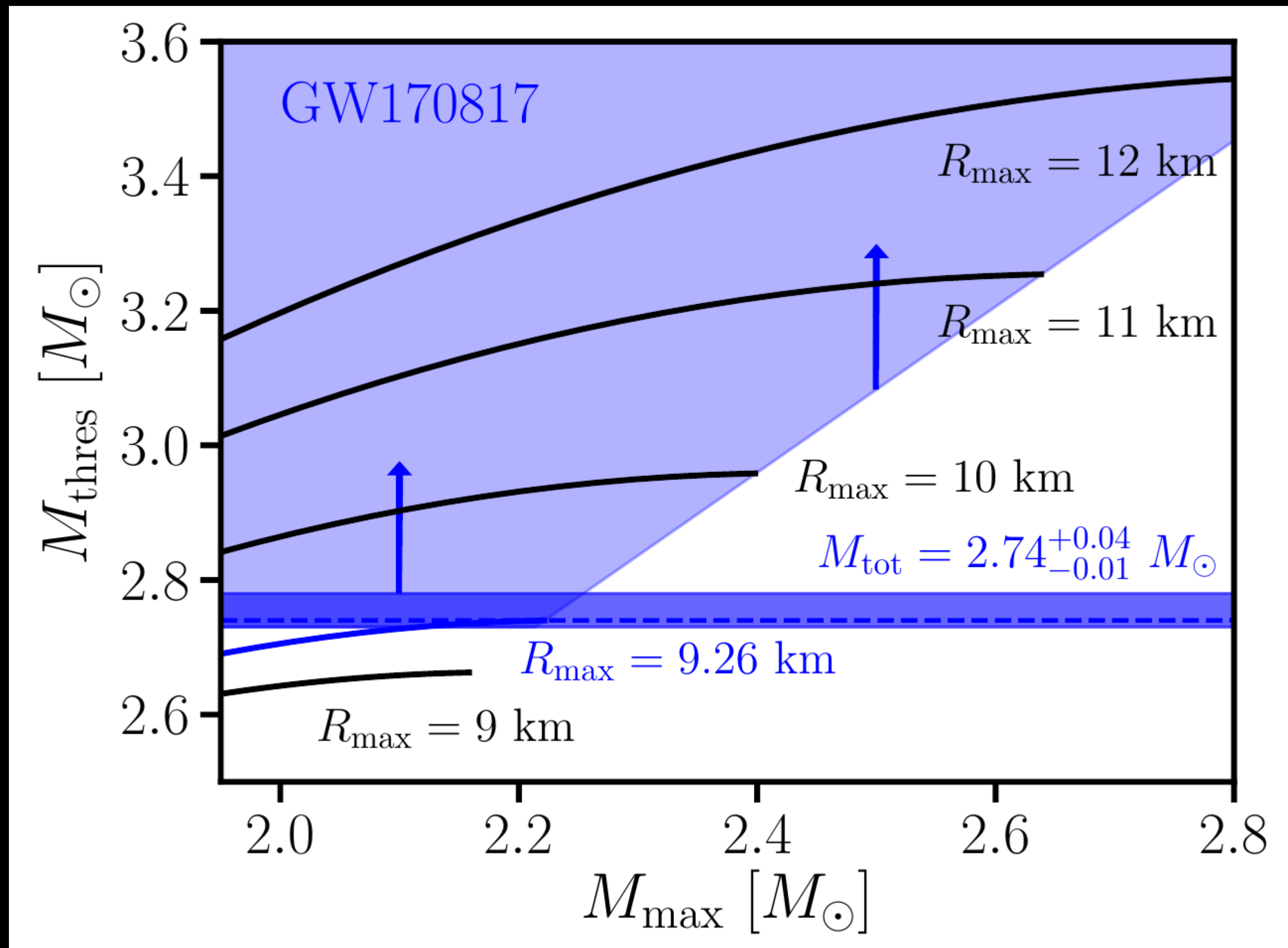


$$M_{\rm thres} = \left(-3.38\frac{GM_{\max}}{c^2 R_{\max}} + 2.43\right) M_{\max}$$

+ causality → $M_{\rm thres} \geq 1.2 M_{\max}$

Bauswein et al. 2017

# NS radius constraint from GW170817

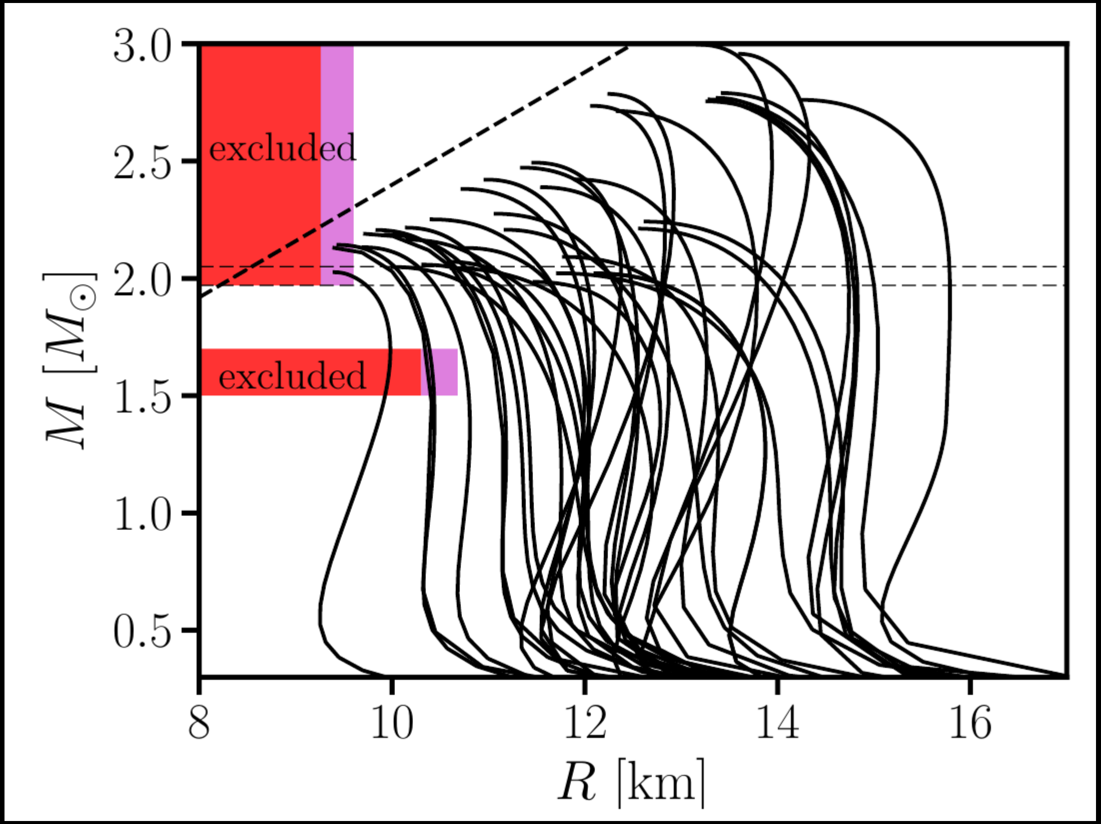


- R16 > 10.7 km
- Excludes very soft nuclear matter

Bauswein et al. 2017

# Discussion

- Binary masses well measured with high confidence error bar
- Clearly defined working hypothesis: delayed collapse

  → testable by refined emission models

  → as more events are observed more robust distinction
- Very conservative estimate
- Empirical relation can be tested by more elaborated simulations (but unlikely that MHD or neutrinos can have strong impact on Mthres)
- Low-SNR constraint !!!

# Future

- Any new detection can be employed if it allows distinction between prompt/delayed collapse
- Low-SNR detections sufficient !!! → that's the potential for the future

  → we don't need louder events, but more

  → complimentary to existing ideas for EoS constraints

# Future detections (hypothetical discussion)

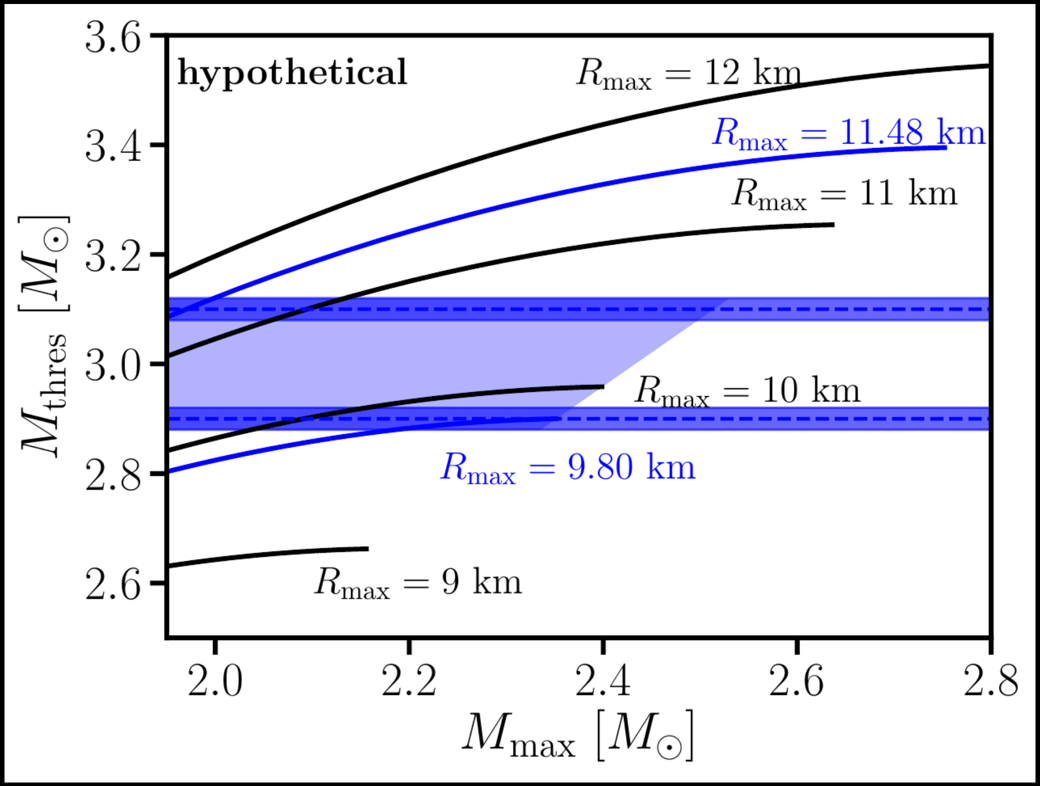


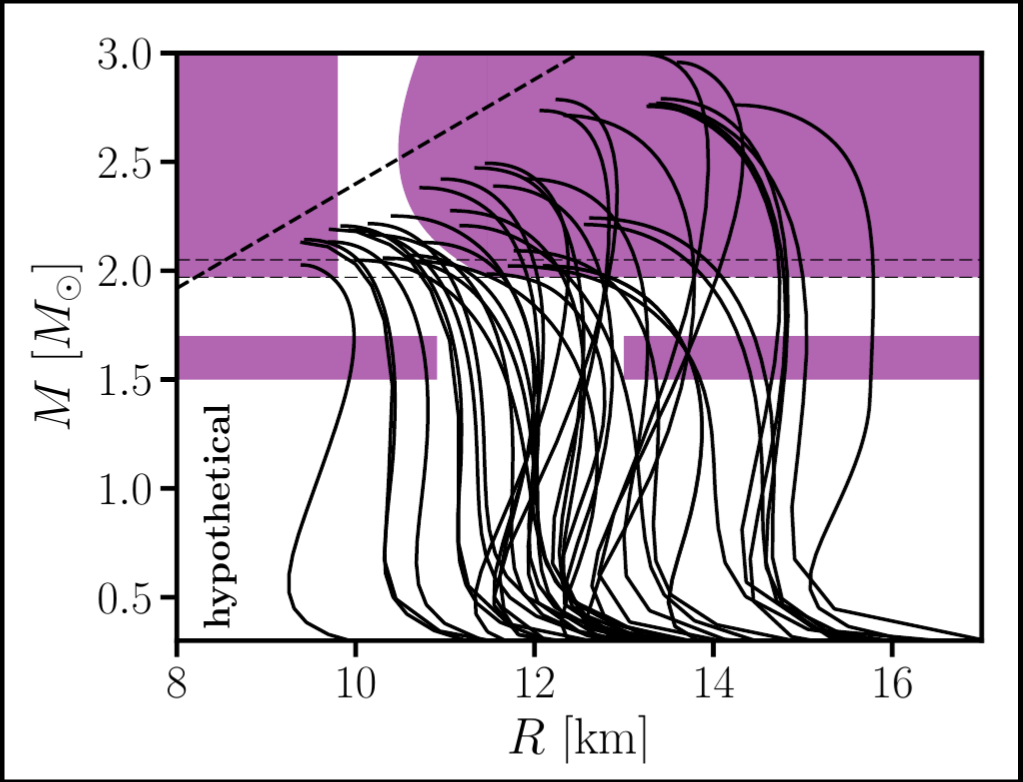


Wow !!!!

Bauswein et al. 2017

# Future plans

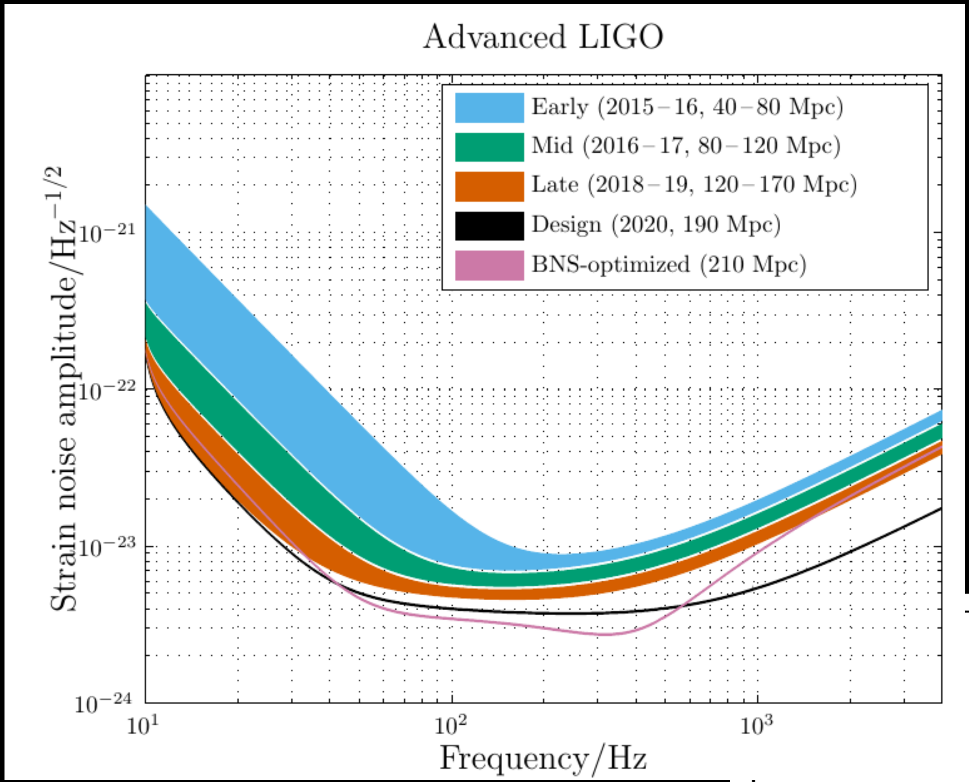


Abbott et al. 2017

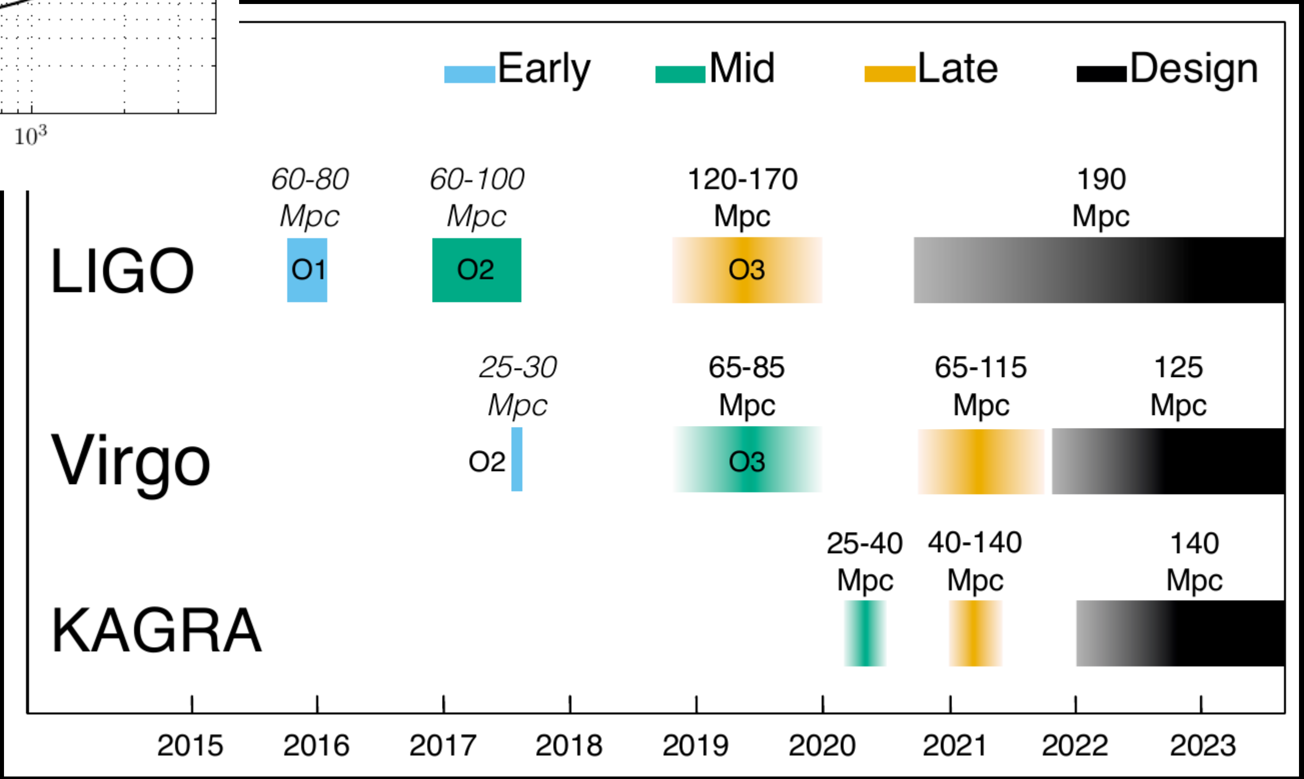

# Semi-analytic model reproducing collapse behavior

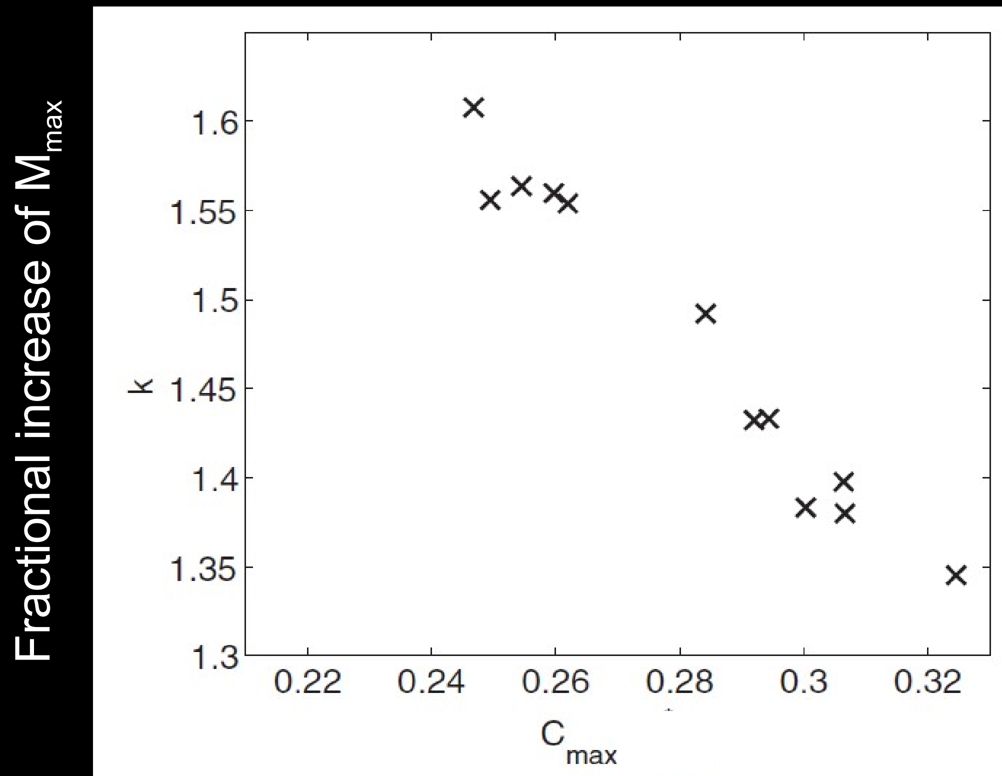


Bauswein et al 2013: numerical determination of collapse threshold through hydrodynamical simulations

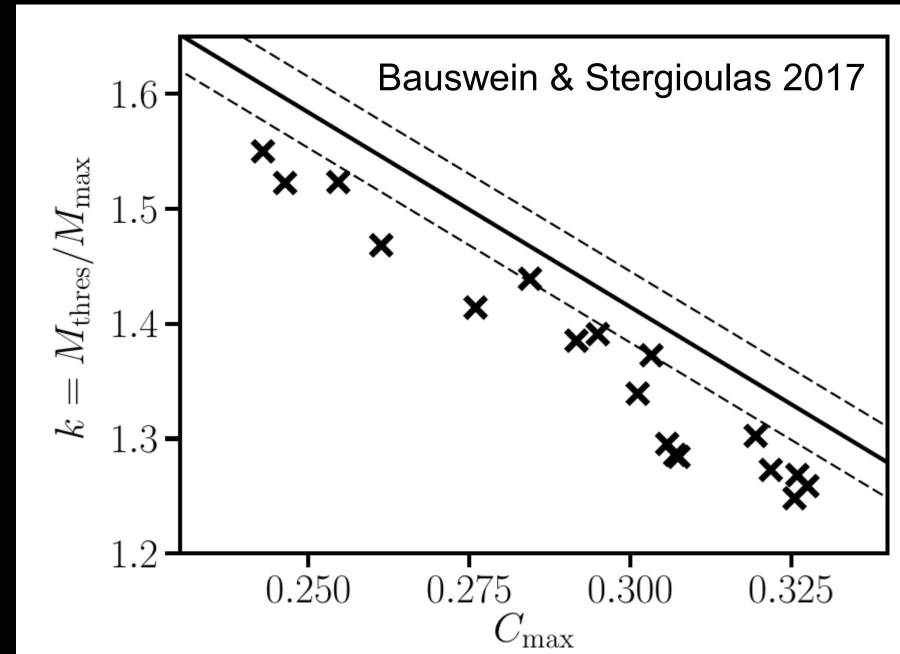


Solid line fit to numerical data

Crosses stellar equilibrium models:

- prescribed (simplistic) diff. rotation
- many EoSs at T=0
- detailed angular momentum budget !

=> equilibrium models qualitatively reproduce collapse behavior

- even quantitatively good considering the adopted approximations

# details of the model

- Stellar equilibrium models computed with RNS code (diff. Rotation, T=0, many different microphysical EoS) => turning points => $M_{stab}(J)$
- Compared to $J(M_{tot})$ of merger remnants from simulations (very robust result) → practically independent from simulations

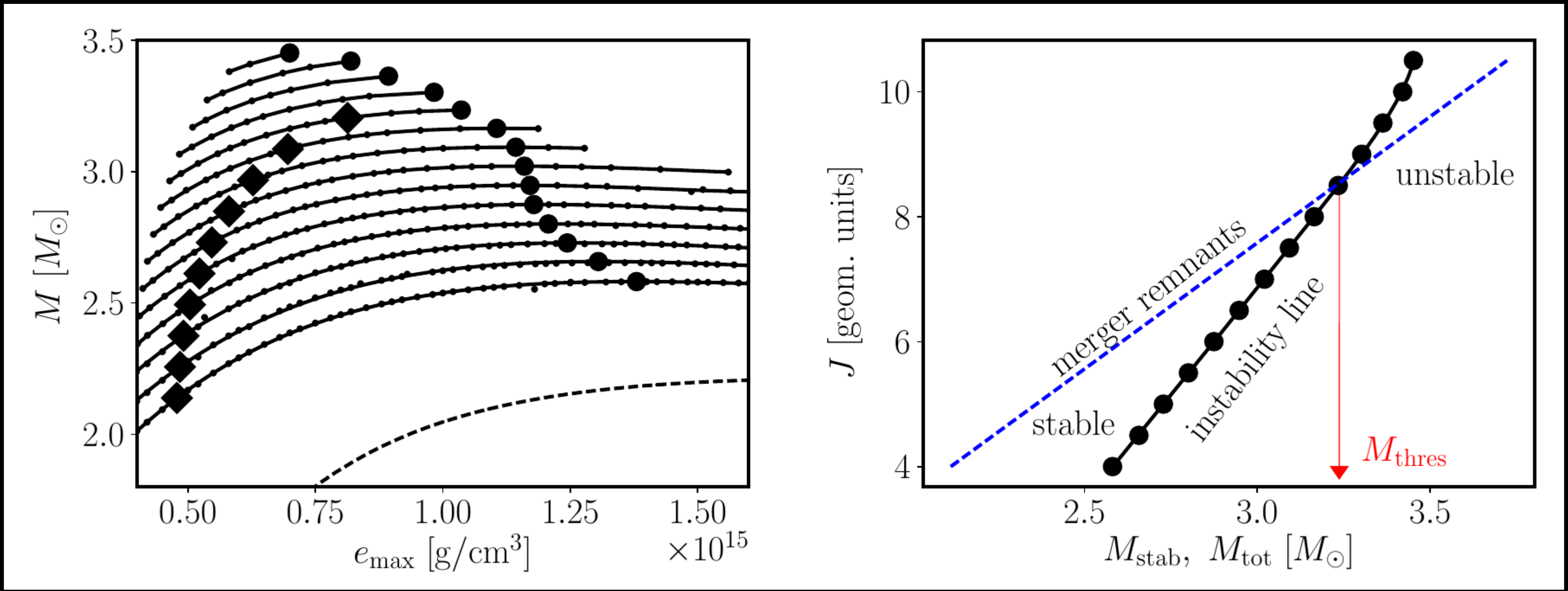


Bauswein & Stergioulas 2017

Maximum mass

- If GW170817 did not form a supramassive NS (rigidly rotating > Mmax)

  → Mmax < 2.2 Msun (somewhat tentative since relying on some assumption)

- Similar arguments presented in other studies

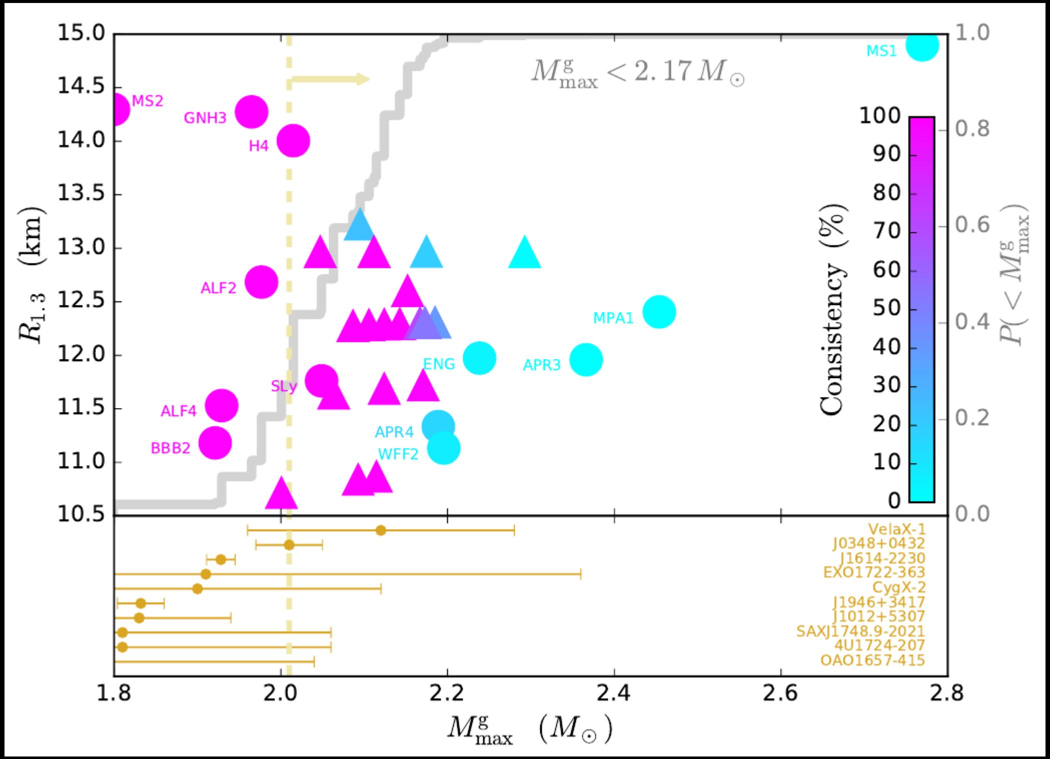


Margalit & Metzger 2017

# Key quantity: Threshold binary mass $M_{thres}$ for prompt BH collapse

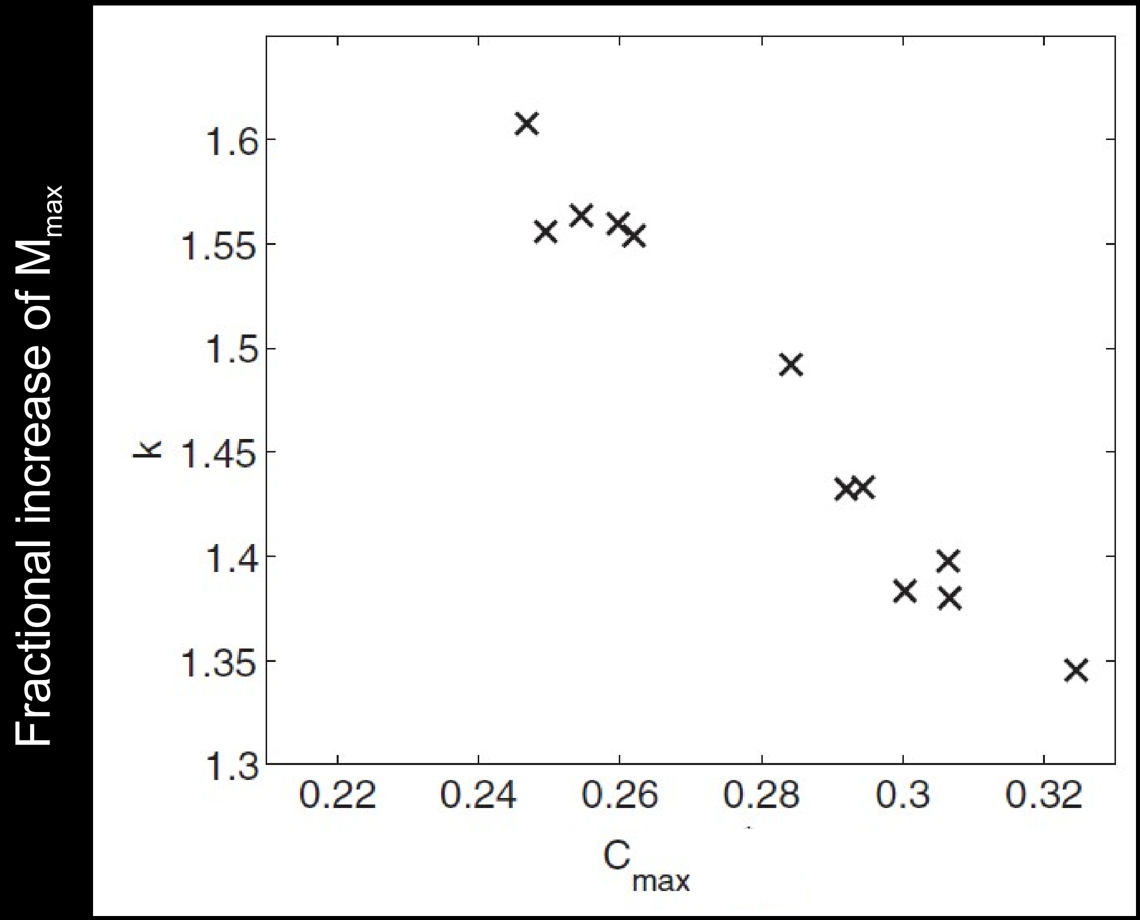


$$M_{thres} = k * M_{max}$$

with $k = k(C_{max})$

$$C_{max} = G\, M_{max} / (c^2\, R_{max})$$

(compactness of TOV maximum-mass configuration)

=> $M_{thres} = M_{thres}(M_{max}, R_{max})$

$$k = \frac{M_{thres}}{M_{max}}$$

← From simulations with different $M_{tot}$

← TOV property of employed EoS

Bauswein et al. 2013

# Constrain $M_{max}$

- Measure several NS mergers with different $M_{tot}$ – check if postmerger GW emission present

  → $M_{thres}$ estimate
- Radius e.g. from postmerger frequency
- Invert fit

$$M_{\mathrm{thres}} = \left( -3.6 \frac{G\, M_{\mathrm{max}}}{c^2\, R_{1.6}} + 2.38 \right) M_{\mathrm{max}}$$

→ $M_{max}$

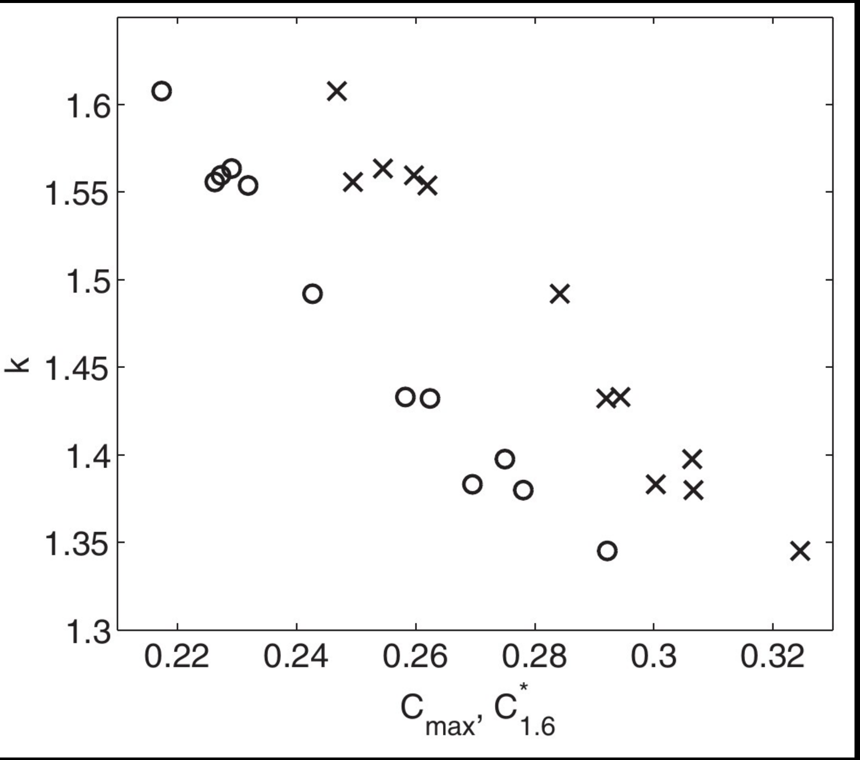


$$M_{\mathrm{thres}} = \left( -3.38 \frac{G M_{\mathrm{max}}}{c^2 R_{\mathrm{max}}} + 2.43 \right) M_{\mathrm{max}}$$

# Alternative: $f_{peak}$ dependence on total binary mass

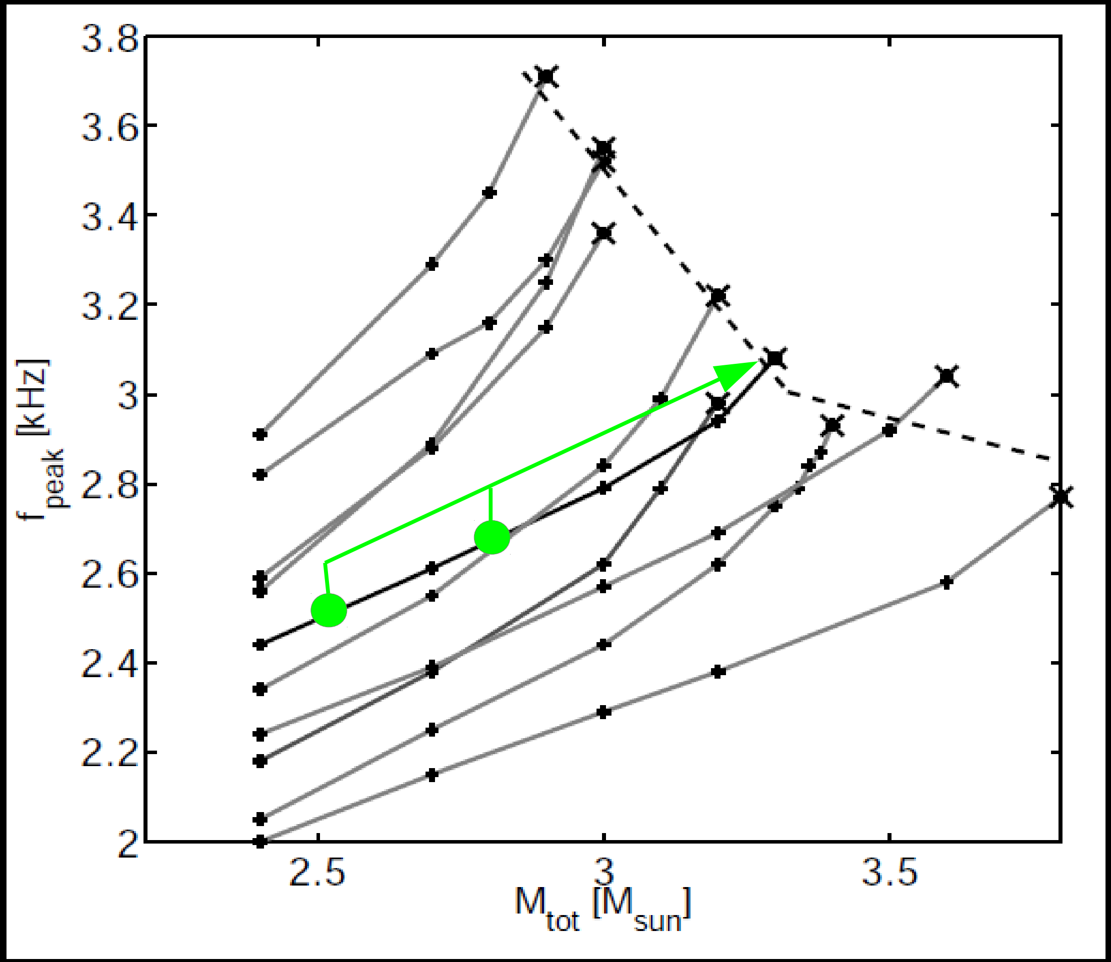


(every single line corresponds to a specific EoS → only one line can be the true EoS)

$$f_{peak} \sim \sqrt{\frac{M}{R^3}}$$

Bauswein et al. 2014

Dominant GW frequency monotone function of $M_{tot}$

Threshold to prompt BH collapse shows a clear dependence on $M_{tot}$ (dashed line)

# $R_{max}$ determination via extrapolation

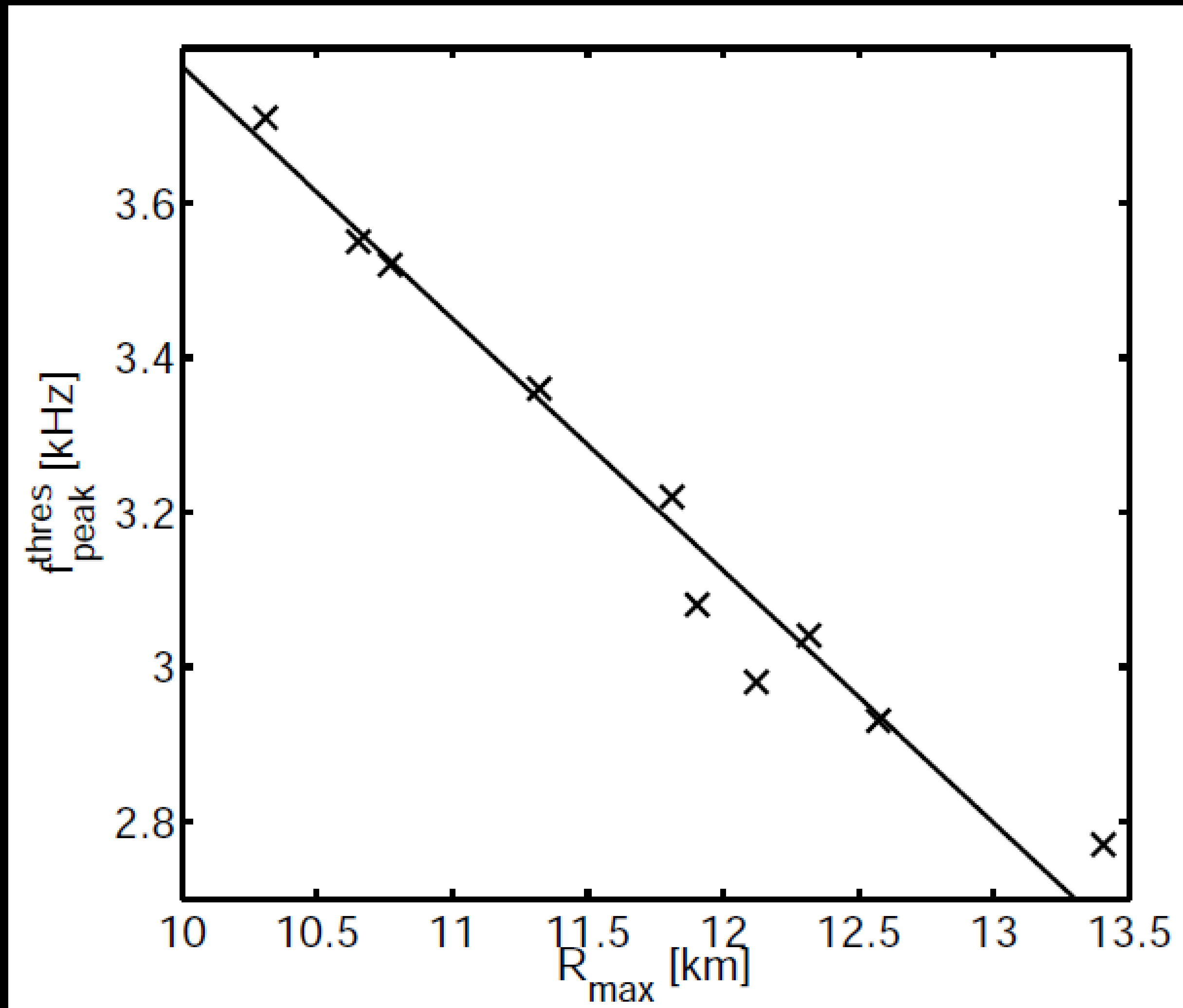


Bauswein et al. 2014

Threshold frequency $f_{thres}$ yields a good estimate of the radius of the TOV maximum mass configuration (a few 100 meters)

# from two measurements of $f_{peak}$ at moderate $M_{tot}$

Maximum-mass TOV properties

by extrapolation of $f_{peak}$ ($M_{tot}$)

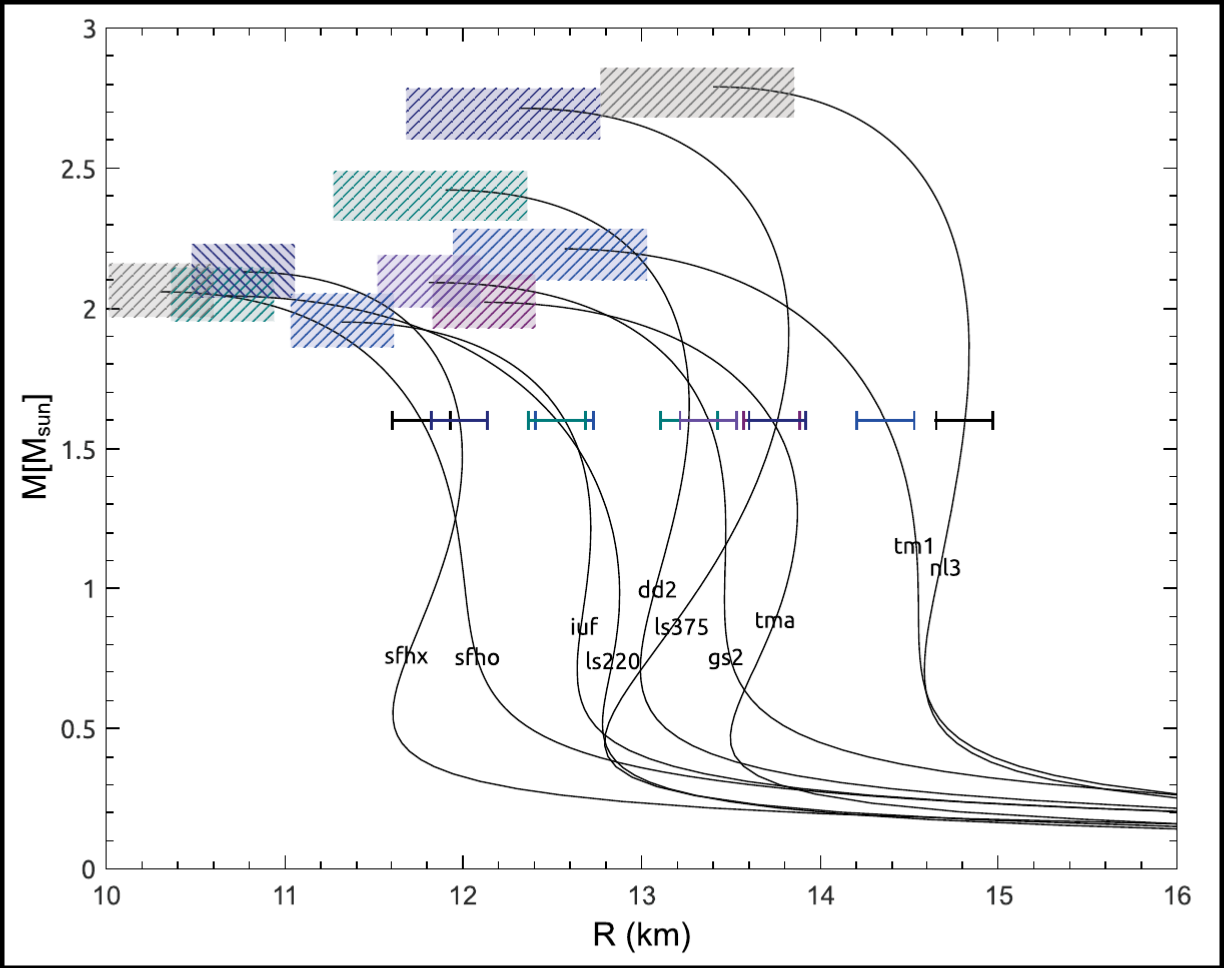


Radius at lower masses from $f_{peak}$

(final error will depend on EoS and extact systems measured)

Note: $M_{thres}$ may also be constrained from prompt collapse directly

Bauswein et al. 2014

# Conclusions

- GW170817 as the first detected NS merger (apart from earlier GRBs) → presumably high rate → promising for futrue detections
- Tidal deformability already constrained

  → excludes very stiff EoS
- Presumable delayed collapse in GW170817 (bright emission → high ejecta mass)

  → rules out soft EoS !
- tentative arguments point to Mmax <= ~ 2.2 ... 2.4 Msun
- Dominant postmerger GW frequency scales tightly with NS radius